A constructive solid geometry-based generative design method for additive manufacturing

Zhiping Wang, Yicha Zhang, Alain Bernard

Version of Record: https://www.sciencedirect.com/science/article/pii/S2214860421001172
Manuscript_b3129d3c7687f7151ff4ef9041876e1d

A Constructive Solid Geometry-based Generative Design Method for Additive Manufacturing

Zhiping Wang[a], Yicha Zhang[b]*, Alain Bernard[a]

[a]*Ecole Centrale de Nantes, LS2N, CNRS UMR 6004, Nantes, France*
[b]*UTBM – Université de Technologie Belfort-Montbéliard, ICB-COMM, CNRS UMR 6303, Sevenans, France*

Abstract

The unique capability of additive manufacturing (AM) to deal with complex geometries drives the traditional topological optimization and lightweight design to a new paradigm. However, AM constraints are still hard to integrate into the optimization procedure, and the multiple conflict design objectives are difficult to handle when making decisions. In addition, the computation cost is usually high. To solve these problems, this paper proposes a new generative design method with a manufacturing validation so that the designer's decision-making is more efficient. This method first uses a CSG (constructive solid geometry)-based technique to generate and represent topology geometries with smooth boundaries and parametric control. Then, a genetic algorithm is used to operate the CSG geometries in order to search for optimal solutions. Finally, a set of finite optimal non-dominated design solutions on the Pareto front are located and presented for the designer's further decision making. The proposed method can generate a large quantity of qualified optimal alternative solutions with smooth geometric boundaries but the computation cost is less. It is promising to design qualified solutions, especially for lightweight structure design, in AM. Several demonstration examples and comparison case studies with existing methods in literature are presented at the end of this paper to show the advantages.

Key words: Generative Design, Constructive Solid Geometry, Topology Optimization, Manufacturability Analysis, Design for Additive Manufacturing

1. Introduction

Additive manufacturing (AM) is defined as a process of joining materials to directly fabricate physical models via 3D model data, usually layer upon layer, as opposed to subtractive manufacturing methodologies [1]. Compared to conventional manufacturing processes, the AM processes give more freedom to designers and engineers to enable them to produce highly complex geometries and material compositions [2, 3]. Since parts are fabricated layer by layer in AM processes, design knowledge, tools, rules, processes, and methodologies have set them apart from traditional manufacturing processes [4]. Therefore, design for additive manufacturing (DfAM), a new research field investigating design methods and tools in AM processes, has emerged to consider the manufacturing constraints within the design process [5-7]. A successful design for AM should be based on the interaction between engineering design, material science and manufacturing. As stated in [4], "The coupling between the design, representation, analysis, optimization, and manufacture still needs to be solved." Due to new design freedom, it provides a high potential to save materials in lightweight application. Hence, lightweight design always has been a hot topic to attract people into the domain of AM. There are generally four main groups of methods for lightweight design in AM [7]. Topology optimization (TO), which searches for a free-form material layout within a given design space in order to obtain the best structural performance, is one of the four methods that explore complex and lightweight shapes with computational automation. Some of the most popular methodologies in topology optimization include the homogenization method, solid isotropic material with penalization (SIMP) and level set methods, etc. Topology optimization has been applied in the design of automotive, aircraft and aerospace structures, for which mass constraints are frequently imposed. To date, commercial TO software, such as Altair, ANSYS, Autodesk Fusion 360, have gained popularity in various industrial applications.

However, existing topology optimization methods still have several limitations that impede industrial application. Firstly, although topology optimization has great potential to exploit the design freedom provided by AM, AM processes cannot always print the obtained structures with successes. This is primarily because AM still has some manufacturing constraints which need to be considered in the topology defining process. Therefore, manufacturing-oriented topology optimization for AM has seen a significant interest since industrial applications can only accept qualified design solutions. In addition, structural optimization problems in industry are usually constrained by multiple conflicting objective functions and boundary conditions in FEA (finite element analysis). Nevertheless, most existing methods can only provide a single topological result for a given optimization problem. Many of the existing optimization methods convert a multi-objective optimization problem into a single-objective optimization, called mono-objective optimization, and obtain one particular solution at convergence. Therefore, these methods naturally eliminate other non-dominant solutions, called the Pareto set, in the solution space. Due to the conflicting nature among the predefined objectives, there is a need of a Pareto-optimal set representing trade-offs for further decision making according to diverse preferences for specific requirements and compromise in engineering applications.

Furthermore, from the perspective of optimization techniques, topology optimization methods are usually classified into two main categories: gradient-based TO and non-gradient-based TO methods [8]. Gradient-based methods rely on the gradient information, called sensitivity, to search for the optimal solutions. They are widely used in the density (SIMP) approach, the level-set approach, topological derivatives, etc. The main reason is that the gradient-based methods can efficiently solve fine-resolution problems with up to millions of design variables by using a few hundred function evaluations [8]. Non-gradient-based TO methods, also called black-box TO [32], usually use evolutionary algorithms and other soft computing techniques to generate near-optimal topologies of mechanical structures. Evolutionary-based TO methods are more flexible for problems without gradient information. Moreover, evolutionary computation applies global search techniques and hence can tend to converge towards a global optimal rather than a local optimal [31]. One of the main challenges that limits the wide use of an evolutionary algorithm in TO is that the elements using fine grid representation causes a great deal of design variables, which limits its effectiveness and convergence [31, 32].

To deal with the limitations of current TO methods, especially evolutionary TO methods for AM as introduced above, this paper proposes a new generative design method which is based on evolutionary computation. In order to reduce the design variables and improve the rate of convergence, a modified CSG (Constructive Solid Geometry)-based geometric representation is applied to define the structure geometry so as to release the potential of multi-objective evolutionary algorithms. With CSG representation, AM manufacturing constraints can be easily embedded into the evolutionary operation. Hence, the optimization procedure can obtain a set of multi-objective Pareto solutions that are valid design solutions for AM. It differs from traditional TO approaches which use a density-based or gradient method to obtain a single local optimal solution with less consideration of AM constraints. This also enables the designer to explore and compare more alternatives along the Pareto front to fit their application requirements when making compromises from multiple predefined objectives. The remaining contents of this paper are organized as follows: the second section reviews the related works with comments; the third section presents the proposed approach in detail; the fourth section gives some examples for demonstration and comparison with existing methods, and the last ends with conclusions and perspectives.

2. Related work

Due to the capability to deal with complexity and reduced manufacturing constraints as compared with conventional manufacturing processes, AM shows that the traditional TO methods can be widely applied. Lightweight design is more attractive than ever. Although AM has gained popularity, it is still a challenge for designers to fully understand the unique capabilities of AM as well as the process-related constraints. Hence, qualitative design rules or guidelines and quantitative design evaluation frameworks were proposed for DfAM [9-11]. These methods can help to obtain a design solution that meets limited AM constraints for manufacturability requirements, but has less optimization. However, to further benefit from AM, design methods involving structural optimization for AM should not only consider manufacturability, but also need

to improve the functional performance of AM parts via quantitative justification, e.g., simulation and calculation, as well as lightweight improvement. As such, designers can exploit more design potential and have more freedom. Therefore, computation-driven TO is widely adopted as a quantitative design tool for AM. The following subsections review the representative works from literature set out in three main categories.

2.1 Incorporating manufacturing constraints into topology optimization

AM processes can bring more design freedom to realize extremely complex geometries, but still have manufacturing limitations or constraints. These should be considered in the topology optimization process to guarantee manufacturability when designing for AM. One of the most important constraints is the support structure for many powder bed based processes, e.g. Selective Laser Melting (SLM). In general, a support structure needs to be designed to sustain the overhang areas during the printing process. Support structure wastes print time and material. In addition, the removing of these structures in the post-processing stage is still challenging and costly. Therefore, design self-support or support-free structures is desirable. Due on the popularity of density-based TO method, most studies investigated self-support structure for TO are based on density filter-based methods. There are two main methods to obtain self-supporting structure in density-based TO methods. A direct method for obtaining a self-supporting structure is to add additional materials to regions that do not meet self-supporting criteria. Leary [12] proposed a density-based support-free structure generation method by changing the optimal geometry to meet the angle constraints. The method is a post-processing approach which alters the mass and performance of the original optimal part. Other research has concentrated on integrating overhang constraints with density-based TO methods. The main idea is to transform AM constraints into a filter that incorporates the characteristics of a generic AM process. A filter-like projection function was introduced by Gaynor and Guest [13, 14]. The projection-based topology optimization scheme can guarantee the maximum printable angle. One of the limitations in the method is that the topology variables are multiple non-linear functions. Hence, it may cause convergence issues for complex design problems. Langelaar [15, 16] proposed a nonlinear spatial filter that imitates the powder-bed-based AM process. The proposed AM fabrication model was defined on a regular mesh. In [17], Langelaar improved the proposed AM filter [15] and integrated the optimization of self-support and the build orientation determination into the density-based TO method. Wang et al. proposed a density gradient-based boundary slop constraint (density filter) method to control the overhang angle. The AM filter proposed by Langelaar [15] was used by several authors [18-22]. Barroqueiro et al. [18] addressed the minimum feature size and overhang angle constraints in a simplified fabrication model using an AM filter. Fu et al. [19, 20] integrated a smooth boundary representation with an AM filter to solve overhang constraints with SIMP. A slightly extended version of the AM filter was used by Thore et al. [21]. Zhao et al. [22] proposed an explicit local constraint for a density-based TO problem. By efficiently detecting the overhang regions using discrete convolution, the number of unsupported elements is required to be zero. Due to the linear sensitivity that only depends on the design density, the method has a higher convergence rate. While some other studies have attempted to design self-supporting structures based on geometric feature-driven topology optimization, such as the Level set method, the Moving Morphable Components (MMC) method [23, 24] and the Moving Morphable Void (MMV) methods [25]. Allaire et al. [26] addressed the self-supporting design using a level set method. They proposed an implicit constraint function based on a simplified model for the manufacturing. However, the method cannot fully eliminate the overhang. Wang et al. [27] proposed a single domain integral form to detect the overhang constraints for a level set method. By comparison with density-based methods, the level set approach can obtain smoother geometrical information of the structural boundary but would encounter more difficulties regarding convergence. MMC and MMV methods establish a direct connection between structural topology optimization and CAD modeling [23]. These methods are different from the traditional TO methods by eliminating materials from the design domain. The optimal topology structure is obtained by using a gradient-based optimization method. Based on the explicit characteristics of MMC and MMV, Guo et al. [28] established and optimized a set of explicit geometry parameters to obtain the self-supporting structure.

Based on the above observations, almost all existing AM-oriented TO methods use gradient-based optimization by using mathematical programming or shape sensitivities to update and drive the geometry topology to optimality. Although the gradient-based methods are efficient with respect with function

evaluations [8], a gradient is not easy to obtain due to the complexity of engineering problems. Compared to gradient based TO methods with local searching, evolutionary-based TO methods are based on evolutionary algorithms which have more potential to identify global optima for multi-objective problems [31]. Evolutionary algorithms can run more efficiently by using parallel computing [8]. In addition, the rapid development of computing hardware, like Graphics Processing Unit (GPU), also opens up new possibilities to accelerate these solvers. The following subsection reviews this category in detail.

2.2 Evolutionary computation for multi-objective topology optimization

In engineering optimization problems, there are large numbers of conflicting objectives, such as obtaining maximum compliance and minimum mass for the final design. Traditional optimization methods usually convert a multi-objective problem into a single-objective problem by converging one particular single solution on the Pareto frontier. Compared to mono-objective optimization problems, the presence of multi-objective optimization problems paves a way to obtain a set of so-called non-dominated alternative solutions, widely known as Pareto-optimal solutions, instead of a single optimal solution for better decision making. Such Pareto-optimal solutions give more options for designers to select the one that best fits their needs and requirements [29]. One powerful method to obtain a Pareto-optimal set is to utilize metaheuristics-based techniques, such as multi-objective evolutionary algorithms, multi-objective particle swarm optimization. Metaheuristics, e.g. randomized black box algorithms can solve problems with non-linear and non-differentiable objectives. Evolutionary algorithms are one type of the popular metaheuristic algorithms. They are biologically inspired algorithms based on the concepts of genotype and phenotype. The phenotype (or individual) is a population of candidate solutions of an optimization problem. The genotype is defined as a set of variables that can be mutated and altered. In evolutionary algorithms, phenotype (solutions) are encoded into the genotype (variables) where operators are used. Eiben and Smith [30] give a definition of representation, "*mapping from the phenotypes onto a set of genotypes*". In geometric topology optimization, the representations for evolutionary computation proposed in [31, 32] are categorized into three types: grid, geometric and indirect representation, as shown in Fig. 1.

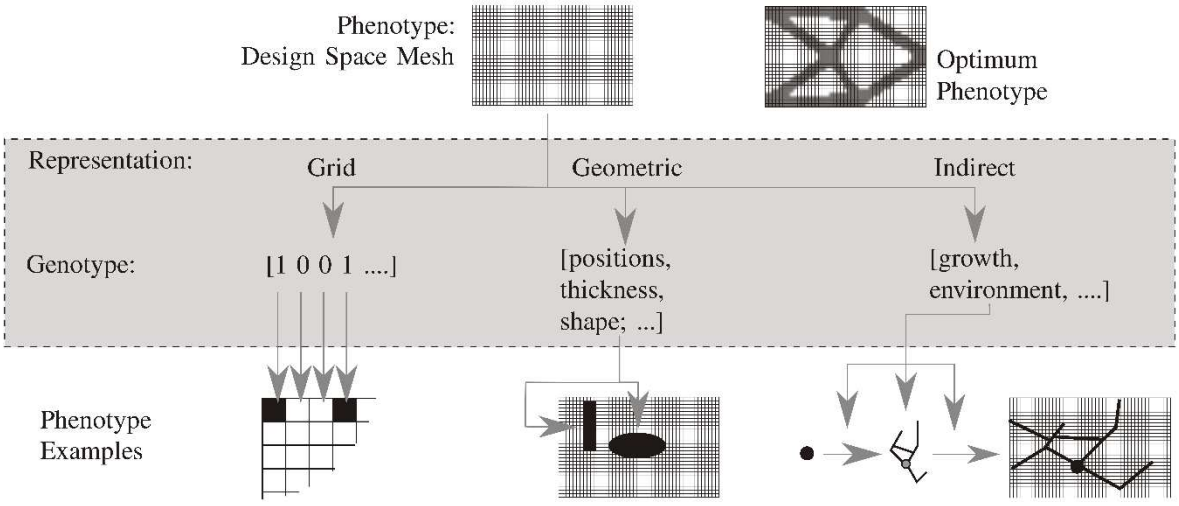

Fig. 1. Three types of representations for evolutionary-based topology optimization [31, 32]

In grid representation, the genotype encodes properties of fixed locations in a grid that decomposes the design space. The representation is applied in density-based topology optimization. In indirect representation, the genotype encodes variable properties of a generative model which implicitly defines material locations or geometry. The Lindenmayer system (L-system) [33, 34], neuro-evolution [35] and compositional pattern producing networks (CPPNs) [36] are applied in order to obtain topology structures. In geometric representation, the genotype encodes properties of a set of fixed or movable shape primitives that define the geometry of the structure within the design space. Properties of the shape primitives are position, shape or thickness, et al. The potential of structural complexity depends on the number of primitives. Voronoi-cells [37], Delaunay-triangulation [38, 39] and the Level set methods belong to the geometric representation.

Although evolutionary-based algorithms are widely used for multi-objective topology optimization [40-42]. they are not sufficient or efficient enough to deal with many thousands of design variables when applied to large-scale optimization problems [29]. Traditional evolutionary-based topology optimization methods, e.g. the density-based method, operate the design space divided into many small elements and uses the gradient information (local stresses and strain energy densities) to improve the search updates. However, large quantities of small elements cause a great deal of design variables that limit its effectiveness and convergence. In order to improve the efficiency and convergence for topology optimization algorithms, a critical issue for evolutionary-based topology optimization method is to reduce the design variables [8, 31]. Therefore, it is essential to choose the suitable topology representation. In grid representations, the structure is represented by fine grid elements (up to several million). Within the vast search space, it is impossible to obtain the convergence to the global optimal within reasonable computational efforts. Compared to grid representations, geometric representations [31] can reduce the dimensionality of the design space significantly. Although many evolutionary algorithms have been applied in topology optimization problems, the manufacturing constraints for AM processes have rarely been mentioned.

2.3 Generative design method

Generative design methods, a set of design exploration methods, are widely known in architectural [43] and industrial design. There are many explanations for generative design methods, including shape grammars [44], L-system, cellular automata [45], etc. In structural design, evolutionary algorithms are usually applied to generate design solutions that are close to predefined objectives and criteria [7]. Instead of focusing on one optimal solution such as traditional TO, generative design can populate a large number of design solutions from the design space for designer's reference and further decision making. Hence, the application of a generative design method for topology optimization may avoid the existing limitations, such as mono-optimal solutions, difficulties in obtaining gradients, etc., of conventional TO methods as discussed above. Recently, a set of commercial software provides new functions of the generative design method for AM processes in their structure design module, such as Autodesk and Altair. However, these tools, based on traditional multi-objective topological optimization, only alters the way of removing materials from the design space to populate alternative solutions, most of which are invalid. Key manufacturing constraints of AM processes have been ignored in the material removing procedure. The result is that these commercial tools usually generate very complex geometries without validation for manufacturing. Hence, designers have to use their own knowledge to evaluate and select the optimal solution from the large number of populated non-valid alternatives, which is quite difficult for operation in design practice. In the academic community, similarly, quite few researchers have considered the manufacturing constraints in generative design algorithms. In [46, 47], a new design methodology using generative multi-agent algorithms for AM process was developed to mimic termite colony behavior. The proposed generative design tool can simultaneously design, optimize and evaluate the manufacturability of an AM concept part. It provided a new method to preserve manufacturability and required functionality. However, the method only takes support structures as the only AM constraint. Recently, a new concept combining generative design with deep learning was provided to explore more design space [48]. The proposed GANs (generative adversarial networks) gave the possibility to embed existing AM process knowledge into generative design methods. However, the method only concentrates on design exploration and generating numerous design solutions without optimization. In addition, it is difficult to evaluate candidate solutions and obtain a large amount of training data.

According to the application of generative design in the architectural design field, generative design is described as a design exploration approach to support designers in automating the design process [43]. In contrast with high design freedom and aesthetic needs in the architectural field, engineering problems in the manufacturing field are usually driven by the performance and manufacturability. Therefore, in this paper, the generative design for AM is defined as a new design process that integrates the specific manufacturing information into the geometry definition procedure and can populate a large quantity of qualified alternative design solutions to meet the application requirements and AM constraints. To cope with this definition and meet the needs of design practice in industry, a new AM-oriented generative design method based on constructive solid geometry (CSG) modeling is proposed. The use of the CSG-based modeling method to construct optimal structures was firstly investigated in [38, 39]. The researchers utilized Delaunay triangulation skeletons to obtain overlapping rectangles and then to generate a final structure via a series of

Boolean operations. However, there are still several limitations for this method. Firstly, the final structure obtained has sharp internal corners where the stress is significantly greater than the surrounding region. Hence, stress concentration is easy to occur. Secondly, manufacturing constraints were not considered and the method was not developed for manufacturing, especially specific AM processes. Inspired by that work, the approach proposed by this paper makes significant improvements by modifying the original method and embedding additional manufacturing constraints for AM process. The following section presents the proposed method in detail.

3. AM-oriented generative design method

The proposed method has two main steps. The first step is the generation and representation of validated topology geometry to meet AM manufacturability, and the second is to populate alternative design solutions and conduct optimization via multi-objective evolutionary algorithm.

3.1 Geometry representation with reduced variables

As introduced above, to reduce the number of design variables and release the potential of evolutionary algorithms, the CSG representation is applied. The detailed steps to generate a CSG geometry topology are described in Fig. 2. One principle difference from other topology optimization methods is that the build orientation is determined before topology optimization. The basic idea in the proposed method is to utilize a set of moving and fixed nodes to obtain Delaunay triangulation skeletons. Then, by allocating a radius to each node, a set of overlapped primitives connected with different nodes can be obtained. Manufacturability analysis and continuum topology validations are then utilized to guarantee the design validity. For a primitive meeting manufacturability analysis, Boolean operators are applied to obtain the final continuum structure. The workflow can be summarized in the following steps:

1. Define the fixed nodes
2. Determine the pre-optimal build orientation
3. Define the variable/moving nodes
4. Generate primitive units
5. Manufacturability analysis
6. Continuum topology validation

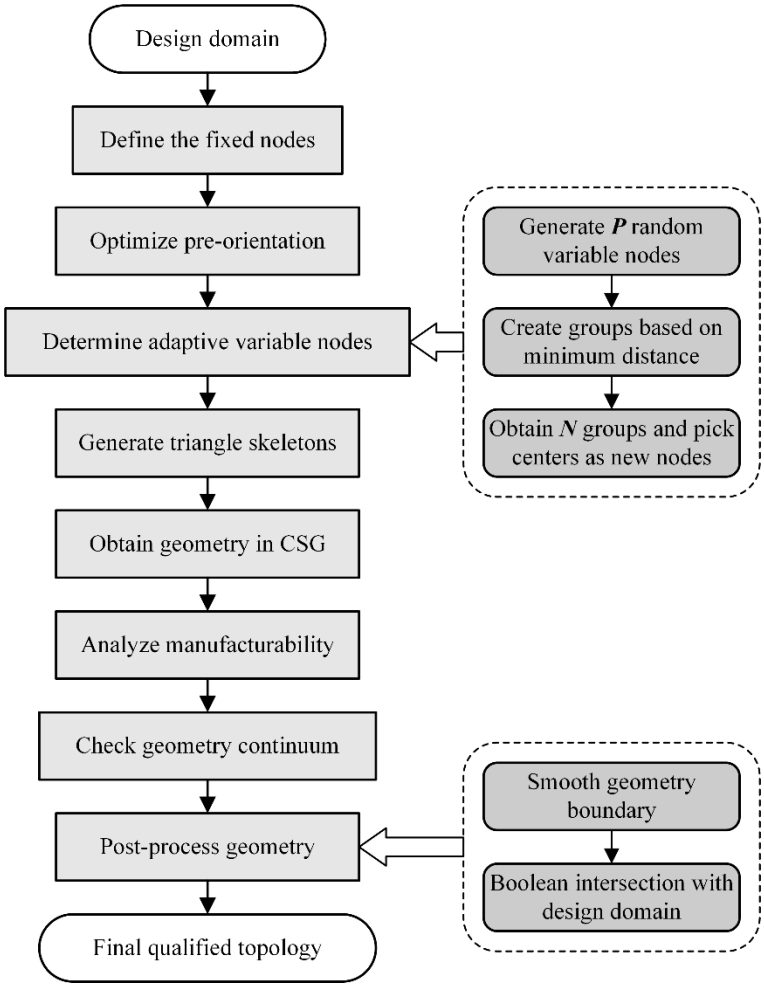

Fig. 2. Flowchart of the generation of qualified AM design solutions with CSG-based geometric representation of the AM-oriented generative design method

3.1.1 Define the fixed nodes

The proposed geometric representation scheme defines the structural topology by position of a set of nodes in the design space. For a design domain as shown in Fig. 3(a), we firstly need to define a set of fixed nodes representing spatial locations where materials must exist. Generally, loading contact points and support boundary limits are regions where fixed nodes are placed. Hence, they are usually on the boundaries of a design domain. Within the design domain, a set of moving nodes, which can be located anywhere, are defined as design variables. Section 3.1.3 below will show how to define these points in the design domain. As shown in Fig. 3(b), green nodes represent the variable nodes and red nodes represent the fixed nodes. Connecting the fixed nodes and the variable nodes by the edges, a topology skeleton can be generated via the use of the Delaunay triangulation algorithm (Fig. 3(b)).

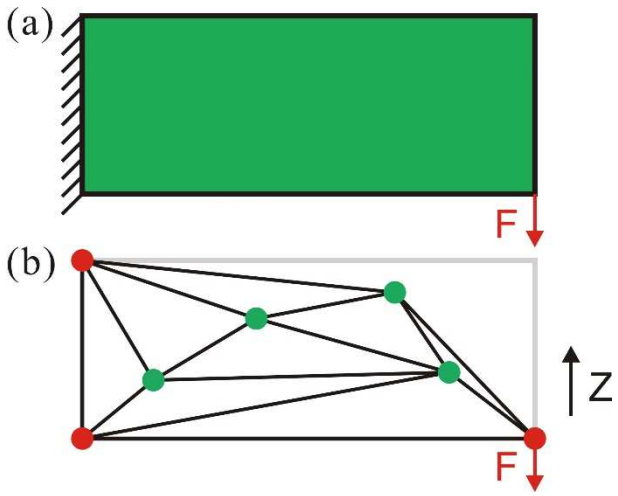

Fig. 3. Node definition for design domain: (a) original design domain; (b) node definition (red nodes represent fixed nodes; green nodes are variable nodes)

3.1.2 Determine the pre-optimal build orientation

Build orientation concerns the direction along which the AM machine deposit materials. It has significant impact on the printing results, such as the final cost, accuracy, and surface roughness of the part as well as the mechanical properties. Hence, it is important to determine an optimal build orientation before any printing [49-51]. There has been a lot of research on build orientation determination for a well-defined CAD model, but much less work on the build orientation in the design stage and TO. In [52], an approach to simultaneously optimize build orientation and part topology was utilized to minimize the amount of supported surface area and support material. However, this work, also including previous research, omitted an important fact that AM processes have specific printable overhang length or bridge length without the need of any support. This length is determined by the material properties and the geometric parameters, e.g. layer thickness and successive inclination angles. Hence, in some conditions of the overhang area, the materials can be supported by themselves. This phenomenon is also called self-supporting. Fig. 4, shows bottom layers of materials supporting upper layers of materials in inclination. In this paper, this method looks at self-supporting and applies it to the pre-build orientation optimization for the design domain. A design domain with a pre-build orientation means the following detail design will respect the orientation constraints. Hence, the build orientation will be integrated in the following TO process from the beginning. Generally, there are two main steps to determine the pre-build orientation for a design domain.

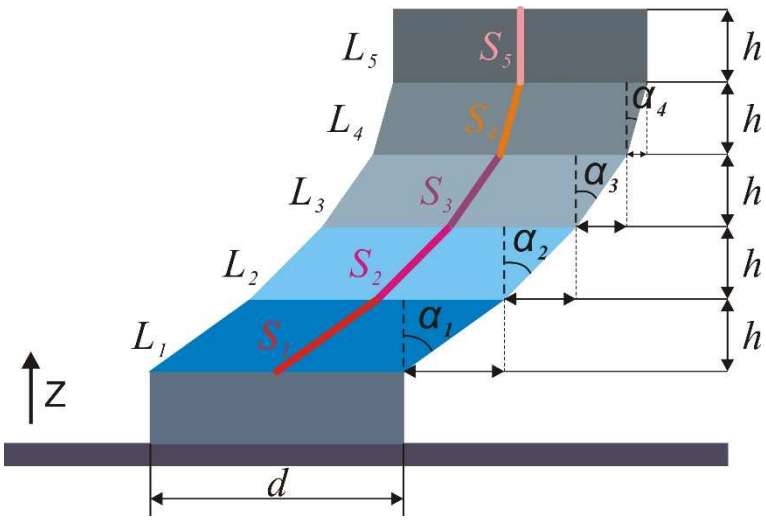

Fig. 4. Overhang downward-facing inclination with different angles and skeleton positions. (h represent the height of each overhang region in build orientation; L_i , S_i and α_i represent ith overhang region, overhang skeleton and overhang angle, respectively.)

Firstly, as the overhang inclination angle directly determines if the overhang region is self-supporting, it is crucial to obtain as many inclination angles as possible to meet self-supporting requirements in the design domain so as to harness the benefits of this phenomenon in AM. Fig. 4 provides a relationship between the overhang inclination angle and the overhang region. In the overhang regions L_i, S_i and α_i represent the corresponding skeleton and inclination angle, respectively. The skeleton angle has a direct impact on the overhang downward-facing inclination angle. Therefore, a transformation relationship between self-supporting primitive and self-supporting skeleton is proposed to help to determine the optimal build orientation. In order to acquire more self-supporting skeletons in the design domain, an objective function for a regular rectangular design domain is formulated as:

$$f_1(\theta) = min(P_x / P_z) \tag{1}$$

Where θ is the rotation angle, P_X and P_Z in Fig. 5 are the projected lengths of the design domain on the X and Z direction, respectively. Mathematically, the objective can be represented by minimizing the proportional value of the projected length of the design domain on the X and Z direction to enable to obtain more self-supporting primitives along the Delaunay triangulation skeleton. Fig. 5(c) and (d) are two examples of the optimal build orientations by using the objective expressed via Equation (1).

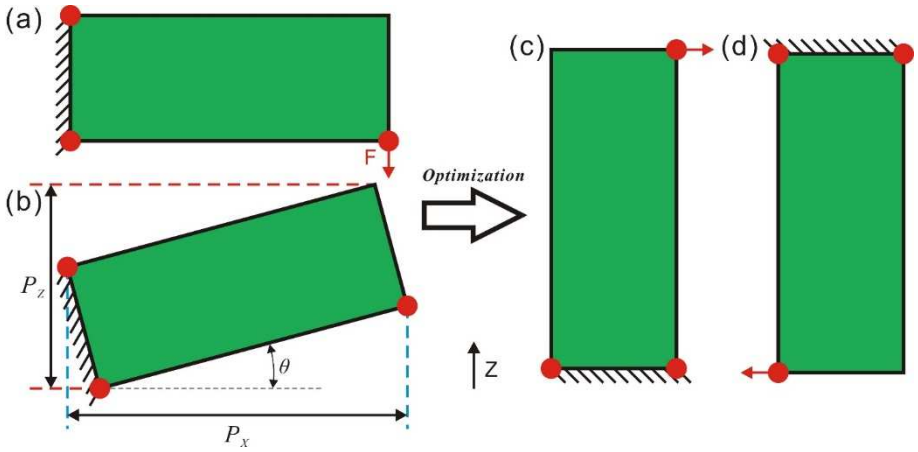

Fig. 5. The pre-optimal build orientation for the design domain

Secondly, in many AM processes, there is a spacing Δ filled by support structures between part bottom and baseplate, as illustrated in Fig. 6. This space is necessary to facilitate the post processing, e.g. removing a part from the base without damage. Hence, this space is also called the mandatory support cost region (base support region between the base and the part [17]). Therefore, the second objective is to minimize the support cost regions. Since this region and its related support volume depend on the pre-build orientation of the design domain and the detailed bottom shape of the part, it would be hard to estimate the exact support volume before the determination of the final topology geometry of the part. However, the projection length of the bottom boundary in the design domain has a positive proportional relationship with the support volume in this support cost region. In this situation, the minimization of the support structure (S_Δ) is converted to minimize the number of fixed nodes that need support. The objective for the rectangular design domain in Fig. 5(a) is given by:

$$f_2(\theta) = min \sum S_\Delta \Rightarrow f_2(\theta) = min \sum N_i (i = 0,1,2,...,m) \tag{2}$$

Where N_i indicates whether *ith* fixed node is the lowest point, where 0 and 1 imply the absence and presence of fixed nodes. Fig. 6(b) is the final optimal build orientation for the illustrative design domain. In this illustrative example, the design domain is a rectangular simple shape and it is easy to identify the optimal pre-build orientation. However, it is necessary to consider the stability of part in printing for large-scale TO problems. From this perspective, the build orientation in Fig. 5(c) is more stable. For real design cases, in particular redesign cases for AM, the design domain with complex boundaries may require the support of other defined objectives for searching. It should be noted that the goal of the pre-optimal build

orientation is summarized as to obtain as many self-supported skeletons as possible in the design domain and to minimize the support cost on the premise of ensuring printing stability.

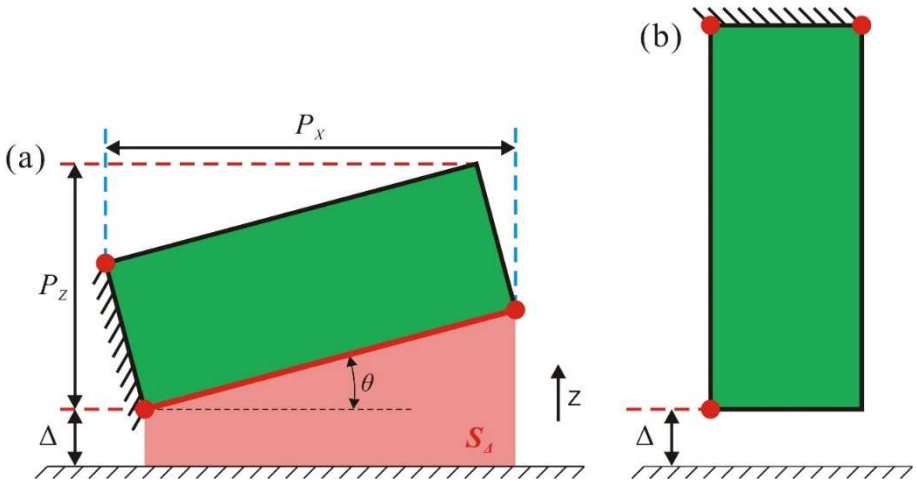

Fig. 6. Determination of build orientation for the design domain via minimizing the support cost region

3.1.3 Define the variable/moving nodes

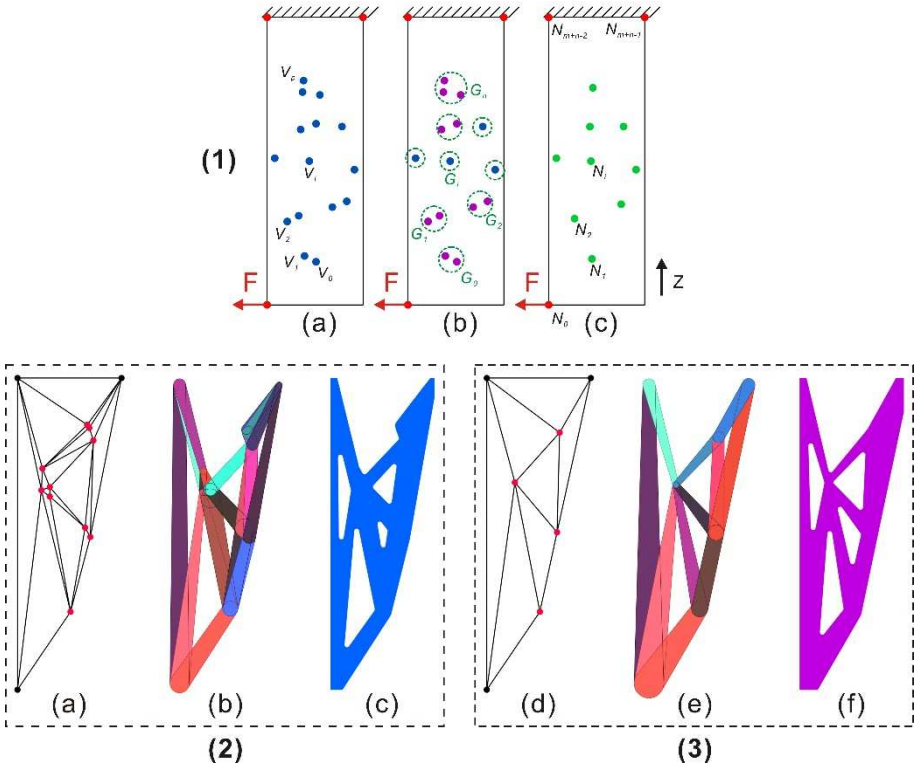

Fig. 7. (1): Adaptive number of variable nodes determination: (a). *p* variable nodes definition; (b). Create group clustering from nearby variable nodes; (c). All nodes definition (*n* variable nodes in green and *m* fixed nodes in red).
(2) and (3): Comparison before and after group clustering analysis. (a, d). Delaunay skeletons; (b, e). manufacturable primitive units; (c, f). final topology shapes.

In the CSG topology generation, geometry skeletons are determined by the number and position of nodes. Fixed nodes are defined by the boundary conditions. Hence, the influence of the number of variable nodes on the triangle skeletons is crucial. Generally, the more points that are within the design domain, the more complex the Delaunay triangulation mesh is. As a result, more CSG volume would be generated based on the Delaunay triangulation mesh. In contrast, if there are fewer moving points defined in the design domain, then a sparse Delaunay triangulation mesh will be generated and less volume would be defined. Both of the

two cases are hard to approach the global optimal solution. Hence, it is critical to define a set of suitable numbers of moving points within the design domain for optimization. To solve this problem, an adaptive method is proposed to determine the optimal number of variable nodes based on the minimum distance. Firstly, a maximum number of variable nodes (shown in Fig. 7(1-a)) are randomly set for generating a sufficiently complex triangular mesh. Then, a clustering analysis is carried out based on the minimum Euclidean distance between variable nodes as shown in Fig. 7(1-b). Finally, the center of each group is determined as a final variable node as shown in Fig. 7(1-c). After adaptive variable node determination, the number of variable nodes is reduced from p to n $(1 \le n \le p)$. If the distance D_{ij} of any two variable nodes is less than the minimum group distance, N_i and N_j are in the same clustering group. We use an average value of the nodes in a group as the radius of new node.

$$D_{ij} \le D_{group} (i, j \in 0,1,2,..., p, i \ne j) \tag{3}$$

An example in Fig. 7(2, 3) shows the Delaunay skeletons, manufacturable primitive units and final topology shapes before and after group clustering analysis. Before clustering analysis, the number of manufacturable primitive units is 25 and most of them are overlapping. However, there are 11 primitive units after group clustering. Group clustering can help reduce the number of the overlapping units. In addition, the number of adaptive variable nodes can be controlled by the minimum group distance. By using group clustering analysis, we only need to define a maximum number of variable nodes and enable to obtain a wide range of Delaunay triangular skeletons with different numbers of variable nodes. This clustering process will be conducted within each iteration loop in the following evolutionary optimization procedure to be introduced in Section 3.2.

3.1.4 Generate unit primitives

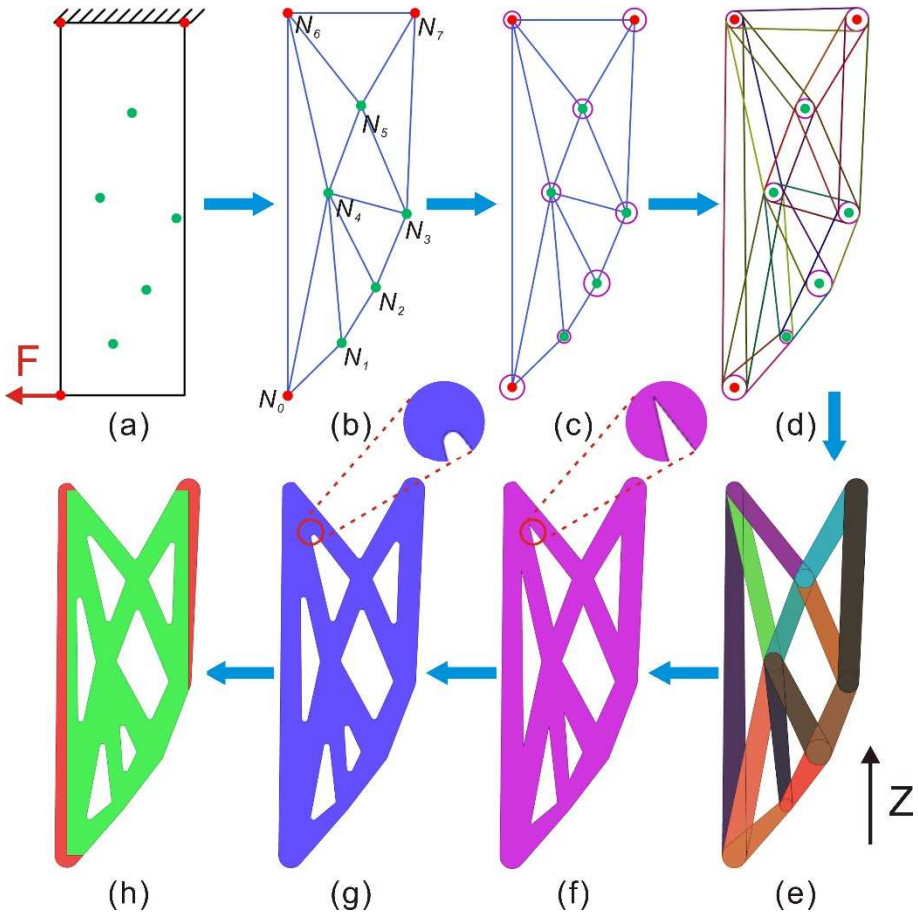

Fig. 8. A schematic illustration of CSG-based topology optimization method: (a) fixed (red points) and variable (green points) node definition; (b) Delaunay triangulation skeleton; (c) assign radius to every node; (d) obtain primitive units; (e) manufacturable original primitive units; (f) perform Boolean union for all units; (g) smooth the shape; (h) obtain the final topology geometry (green color) by performing Boolean intersection operation in the design domain.

Once the design domain orientation is determined, the following step is to generate alternative topology geometries within the design domain. There is a need to give a generic representation of topologies. In this method, as said above, CSG generation and representation are adopted. Fig. 8 presents an illustration to explain the geometry generation and its post-processing. In Fig. 8(a), the optimal build orientation is determined, fixed and moving nodes are defined in the design domain. All defined nodes are sorted by the position of those nodes that node N_{i-1} is always below node N_i. If the z positions of node N_{i-1} and node N_i are equal, node N_{i-1} is always located to the left of node N_i. In other words, nodes are arranged in ascending order of position values (first z, then x). The skeleton of geometry (Fig. 8(b)) is formed by using Delaunay triangulation algorithm. The triangulation returns the upper triangular matrix T_{ij} ($T_{ij}(i, j \in [0,1,..., p\text{-}1], i \neq j, p = m+n)$), as shown in Fig. 9, where 0 and 1 imply the absence and presence of connection between nodes i and nodes j, respectively. Then, every node is assigned one radius variable to generate a corresponding circle, as shown in Fig. 8(c). In Fig. 8(d), the tangent lines are created from each skeleton edge with the corresponding circles. Then, the manufacturability of each primitive unit is analyzed by calculating the slope and length of the first tangent line for every primitive unit. The detail of manufacturability analysis will be explained in the next subsection. The manufacturable primitive units are shown in Fig. 8(e). In Fig. 8(f), the Boolean union is operated to obtain an initial topological structure. In order to avoid the sharp angles or corners causing stress concentration, the boundary of the initial structure is rounded down to r_0 as shown in Fig. 8(f) and (g). The last step is to remove the material (red color in Fig. 8(h)) outside the design domain using the Boolean intersection operation. The final topology structure (green color in Fig. 8(h)) is obtained by a set of nodes and radius represented by p and r.

$$
\begin{array}{c}
 \quad N_0\ N_1\ N_2\ N_3\ N_4\ N_5\ N_6\ N_7 \\
\begin{matrix} N_0 \\ N_1 \\ N_2 \\ N_3 \\ N_4 \\ N_5 \\ N_6 \\ N_7 \end{matrix}
\begin{bmatrix}
0 & 1 & 0 & 0 & 1 & 0 & 1 & 0 \\
 & 0 & 1 & 0 & 1 & 0 & 0 & 0 \\
 & & 0 & 1 & 1 & 0 & 0 & 0 \\
 & & & 0 & 1 & 1 & 0 & 1 \\
 & & & & 0 & 1 & 1 & 0 \\
 & & & & & 0 & 1 & 1 \\
 & & & & & & 0 & 1 \\
0 & & & & & & & 0
\end{bmatrix}
\end{array}
$$

Fig. 9. Upper triangular matrix representing the connection between nodes/skeletons for the given example

In contrast to traditional topology optimization approaches where structures are represented either by element density or nodal values of a level set function, with the CSG-based approach, a set of dynamic primitives is adopted as basic geometric blocks. These primitives are allowed to move, deform, overlap and merge freely in the design domain by changing the design variables (of the fixed and variable nodes with their assigned radius). The structure topology can be optimized by moving the nodes' positions and changing their radius. The method provides a new paradigm for topology optimization in a generative way (generate geometric volume in an additive way and control with parameterization). This method is convenient for the integration of manufacturing constraints in order to adjust the generated parametric alternative solutions with smooth geometric boundaries. Hence, as discussed above, it has great potential to solve some of the current challenges in the topology optimization domain. The following subsection presents the integration of manufacturing constraints for manufacturability analysis.

3.1.5 Manufacturability analysis

To ensure all the generated topology structures are valid for printing, manufacturability analysis should be performed in the TO process. Due to the convenience of parametrization, the minimum printable shape feature size, maximum overhang angle and length can be well embedded. The flowchart presented in Fig. 10 below shows the manufacturability analysis procedure in the proposed CSG-GD method. With the aim that it should be applied at a generic level, this paper focuses on two principle factors, minimum printable feature size and a feasible self-supporting structure, from the perspective of manufacturability.

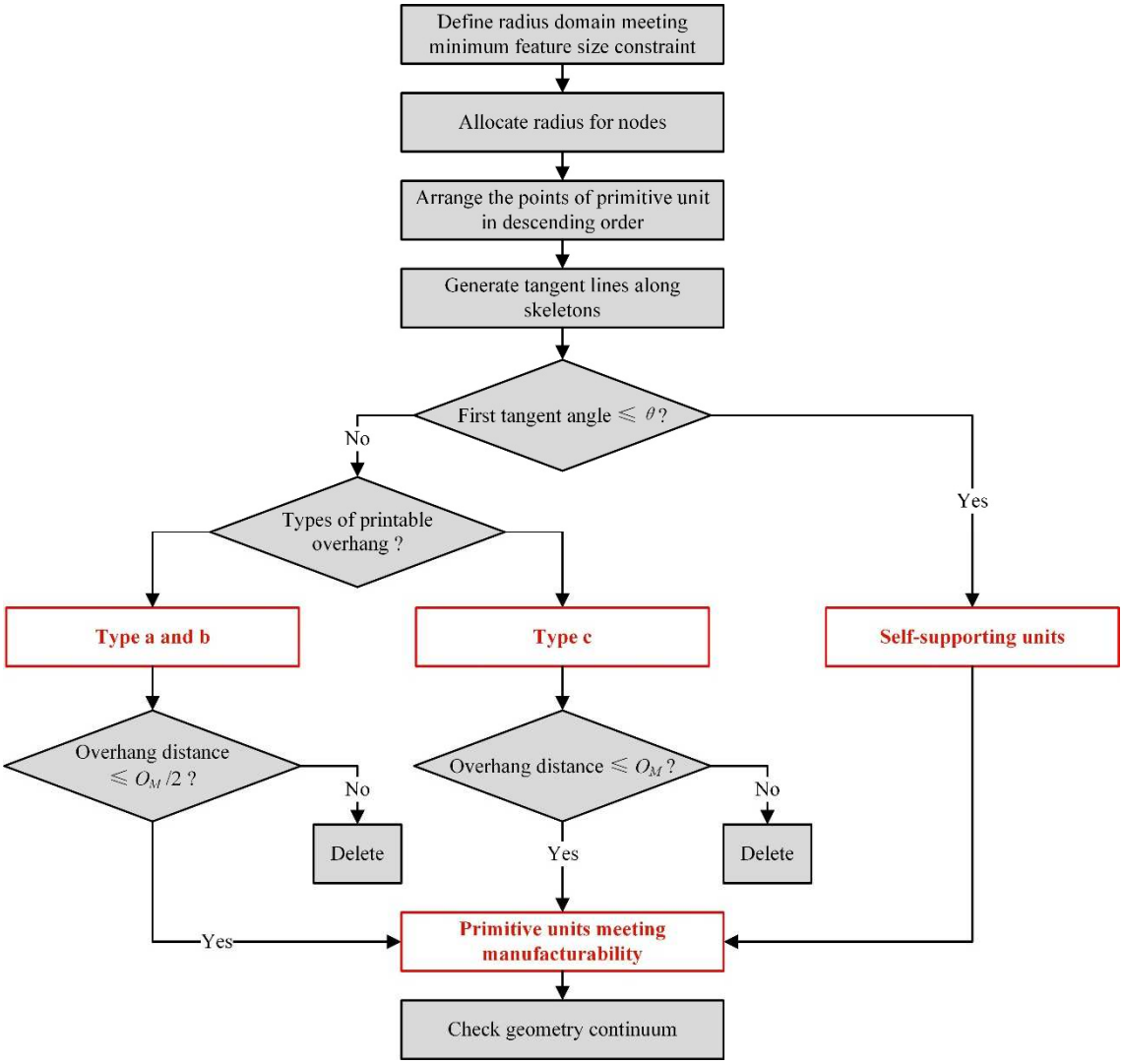

Fig. 10. Flowchart for manufacturability analysis for the CSG-GD method

1. Minimum printable feature size

Minimum printable feature size concerns the minimum shape feature that can be achieved and controlled by AM processing. Different AM processes have different printable size limitations. This size can be obtained via process benchmarking. With a value of this size, the proposed method can easily integrate the minimum size constraints by defining the range of radius r to control the CSG geometries. Considering the nodes appearing on the boundary, the minimum feature size should meet the following constraint:

$$r_{min} \geq 2r_{mfs} \tag{4}$$

In Equation 4, r_{mfs} denotes the minimum feature size constraints, r_{min} represents the minimum radius of nodes.

2. Feasible self-supporting structure

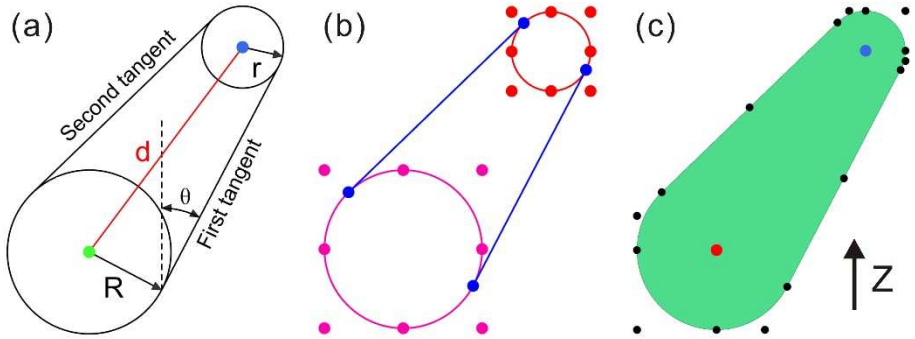

Fig. 11. Primitive unit shape along Delaunay triangulation skeleton: (a) two external tangents along Delaunay triangulation skeleton. (b) parametric geometric control points for subparts of a primitive unit before Boolean union. (c) parametric geometric control point for primitive unit after Boolean union operation

As discussed in the previous section, especially for powder bed-based AM processes, a critical issue for self-supporting structures is to control the inclined angles of structural components. A maximum overhang angle is required to ensure that the design can be produced without the need of any supporting structure. In the CSG-based generative design method, the requirement of a self-supporting structure can be met by giving an angle constraint for controlling every primitive shape. Fig. 11 illustrates an example that the primitive unit is obtained along the Delaunay triangulation skeleton. Fig. 11(a) represents two external tangent lines created by two circles defined by points, moving notes or design variables, on both sides of the skeleton. From a geometric perspective, two tangent lines and circles are determined by control points (blue points as shown in Fig.11(b)). Fig. 11(c) shows a primitive unit with updated geometric controlling points generated by conducting a Boolean union operation. Regarding the manufacturability of the final topology shape, the feasible self-supporting property of every primitive unit can be expressed by a set of parameters related to the tangent lines as shown in Fig. 12 on the XOZ plane. *Z* represents the build orientation in printing.

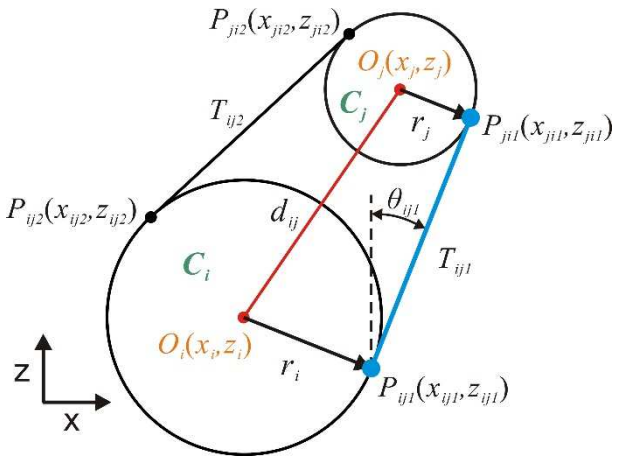

Fig. 12. Detailed definition for points and tangent lines of a primitive unit

The distance between two nodes (O_i and O_j) on the skeleton is

$$d_{ij}=\sqrt{(x_i-x_j)^2+(z_i-z_j)^2} \tag{5}$$

Where (x_i,z_i) and (x_j,z_j) are the centers of circles, C_i and C_j, with radius r_i and r_j respectively. The first tangent line T_{ij1} and second tangent line T_{ij2} always satisfies the following inequality function:

$$z_{ij1}\le z_{ij2} \tag{6}$$

Where (x_{ij1},z_{ij1}) and (x_{ji1},z_{ji1}) are the intersection points between first tangent line T_{ij1} and two circles, C_i and C_j, respectively. (x_{ij2},z_{ij2}) and (x_{ji2},z_{ji2}) are the intersection points between second tangent line T_{ij2} and two circles, C_i and C_j, respectively. The mathematical equation of tangent lines is defined as:

$$T_{ijk}:\frac{z-z_{jik}}{z_{ijk}-z_{jik}}=\frac{x-x_{jik}}{x_{ijk}-x_{jik}}(k=1,2) \tag{7}$$

$P_{ijk}(x_{ijk}, z_{ijk})$ is the intersection point of C_i and the kth tangent line defined by C_i and C_j $(k=1,2)$. Hence, the overhang angle θ_{ij} denotes the angle between build orientation Z and first tangent line T_{ij1}. It can be shown as the following:

$$\theta_{ij} = \arctan \frac{\left| x_{ij1} - x_{ij2} \right|}{\left| z_{ij1} - z_{ij2} \right|} \tag{8}$$

As can be seen from Eq. (8), the advantage of the present formulation is that the self-supporting requirement can be achieved by introducing several explicit geometry constraints. The first tangent line is always denoted as the tangent that is on the inclination side of the primitive unit. Hence, this illustration is similar for the symmetric case as compared to the current case in Fig. 12.

The existence of the first tangent line is closely related to the values of the distance d_{ij} and the radius corresponding to the center of circle. Tab. 1 below lists all geometric relationships between the two circles on both sides of the skeleton. These relationships can be used as rules to evaluate the manufacturability of primitive unit via the calculation of inclination angles using Eq. (8).

Tab. 1 Five kinds of primitive units defined by two circles on both sides of the Delaunay triangulation skeleton

No.	Relationship between circles	Geometric domain	Primitive unit	First tangent line exists?
1	$d > \left| R+r \right|$	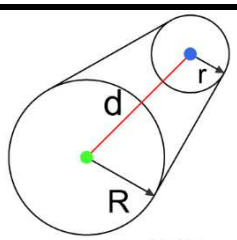	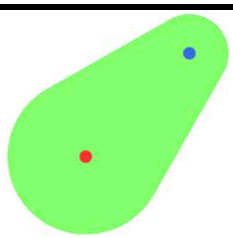	Yes
2	$d = \left| R+r \right|$	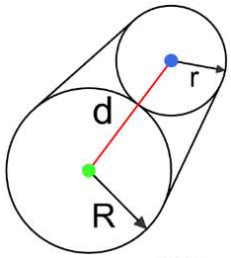	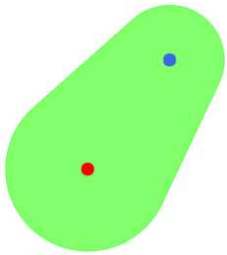	Yes
3	$\left\| R-r \right\| < d < \left\| R+r \right\|$	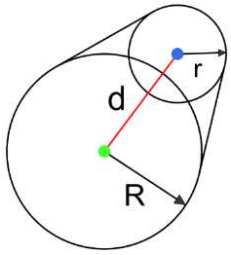	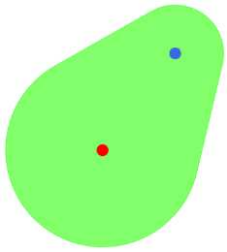	Yes
4	$d = \left\| R-r \right\|$	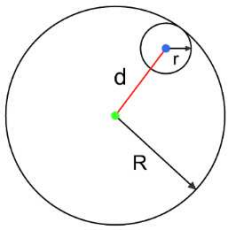	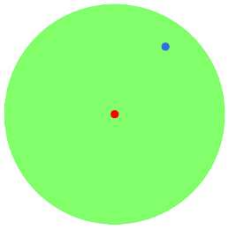	No
5	$0 \le d < \left\| R-r \right\|$	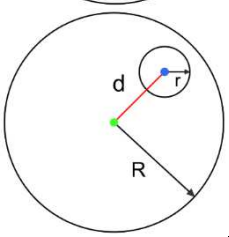	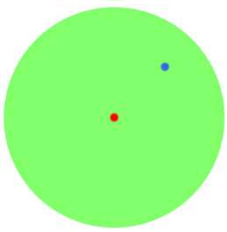	No

As discussed above, most existing self-support TO methods only control the overhang inclination angle to less than a predefined maximum overhang angle value. However, the maximum overhang angle is not the only factor that defines the self-support structure. The printable overhang distance also plays a key factor in guaranteeing self-supporting manufacturability. Therefore, this factor should be included in the TO process. For example, in the SLM processes, the support point respecting the maximum bridge printing length of process capability can provide a stable support for local overhang regions and avoid any surface collapse in printing. This factor was considered for the support structure design in [53], where support points were carefully selected to support the overhang regions. An illustrative example to explain this factor is described in Fig. 13, where the printable bridge length with different values of the SLM process was investigated in [54, 55]. It is clear that small overhangs can be printed when the bridge size is less than a certain overhang distance. Hence, it is essential to consider the maximum overhang angle and the printable overhang distance simultaneously in developing a self-supporting structure.

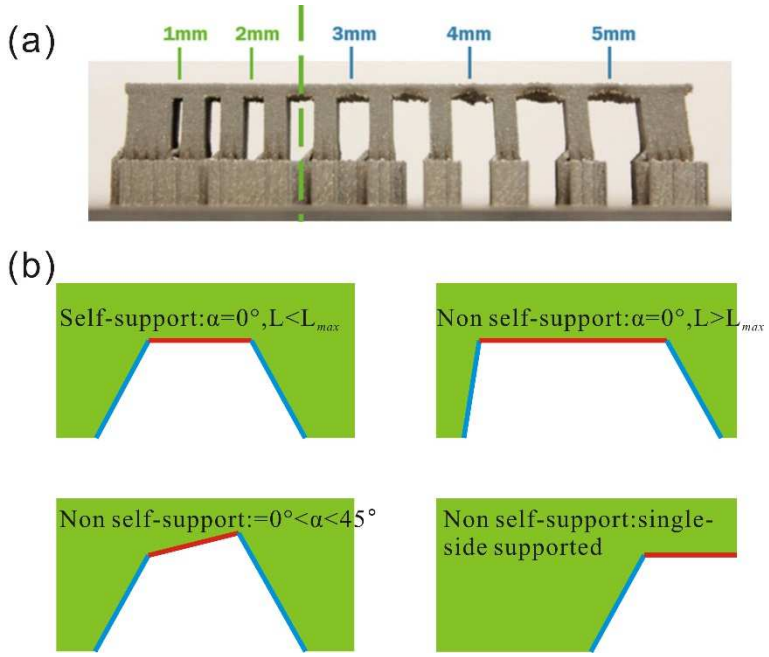

Fig. 13. (a). Effect of unsupported bridge for metal 3D printing [54] and (b). Self-support bridge guaranteeing manufacturability [55]

Based on the previous work, the proposed method in this paper defines three types of printable self-support/overhang structure conditions to guarantee the manufacturability as shown in Fig. 14.

Situation 1: The overhang angle θ is large than the maximum overhang angle θ_M and the horizontal overhang L_H is less than half of the maximum overhang distance $O_M/2$.
(a). Both lower sides of the overhang are self-supported.
(b). The one lower side of the overhang is self-supported.

Situation 2: The overhang angle $\theta \approx 90^\circ$ and the horizontal overhang L_H is less than the maximum overhang distance O_M.
(c). Both sides of the overhang are self-supported.

In essence, type (c) is subordinate to type (b). The connected non-self-supporting overhang should be represented as a whole overhang and then manufacturability needs to be analyzed.

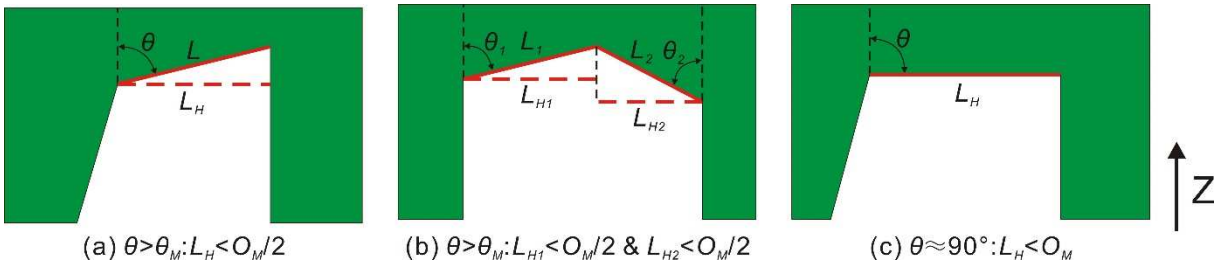

Fig. 14. Three types of printable overhang where the overhang angle is larger than the maximum overhang angle

With the parametric characteristic of the proposed CSG-GD method, it is easy to control these factors simultaneously as discussed above. In Fig. 15. N_i, N_j and N_k are defined fixed or variable nodes. $T_{ij}(P_{ij}P_{ji})$, $T_{kj}(P_{kj}P_{jk})$ corresponds to the first tangent lines of non-self-supporting primitive units, respectively. Blue and green primitive units dictate self-supporting structures; grey and orange primitive units represent non-self-supporting structures.

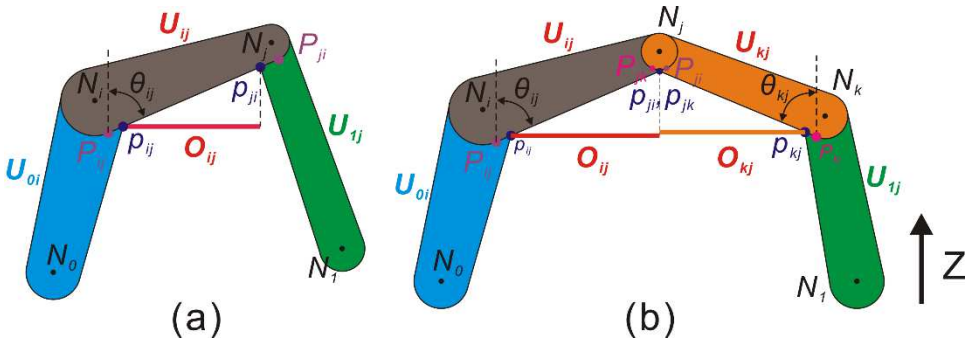

Fig. 15. Overhang distance representations for the proposed CSG-GD method

In Fig. 15(a), a non-self-supporting primitive unit U_{ij} is connected to two self-supporting units, U_{0i} and $U_{1,j}$. This type belongs to the situation 1-(a). In Fig. 15(b), the lower sides of two interconnected non-self-supporting structures are connected to two self-supporting structures, respectively. The maximum overhang distance constraint should satisfy the following mathematical expressions at the same time:

$$\begin{cases} t_{ij}\sin\theta_{ij} \le \dfrac{O_{max}}{2} & (\theta_{ij} > \theta_{max}) \\ \sum t_{ij}\sin\theta_{ij} \le O_{max} \end{cases} \tag{9}$$

In Equation 9, $t_{ij}(p_{ij}p_{ji})$ represents the overhang distance of a non-self-supporting primitive unit U_{ij}. θ_{ij} denotes the overhang angle. O_{max} and θ_{max} are the maximum overhang distance and maximum overhang angle, respectively.

3.1.6 Continuum topology validation

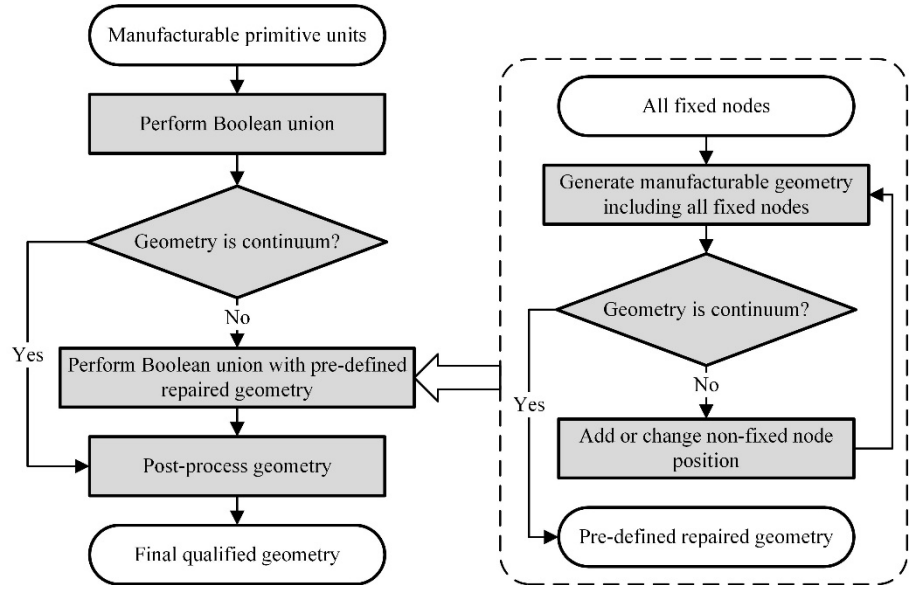

Fig. 16. Flowchart of continuum geometry validation and repaired geometry generation

As discussed above, the initial topology skeleton is defined by the Delaunay triangulation algorithm. A manufacturability analysis is performed to obtain the manufacturable primitive units. However, since the manufacturability analysis is conducted to check each primitive unit before the Boolean operation in the post-processing step, which may cause discontinuity of invalid topologies, hence there is a need to check the volume continuum after the Boolean operation and other post-processing operations for the geometries. To check the connectivity of the topology structure, it is necessary to ensure all the fixed nodes are in the design domain and the topology structure is a continuous volume. Fig. 16 gives a flowchart of continuum topology validation and repaired geometry generation.

In the geometry continuum check, there are usually two circumstances for an inconsistent topology: 1) not all the fixed nodes are connected to the continuum structure. 2) there are two or more disconnected topology structures. Under these circumstances, the inconsistent topology structure must be detected and repaired. One solution is to delete these inconsistent topologies, but this may reduce much of the original solution space. Hence, a continuum geometry repair approach is employed to detect and repair the geometry. In [38], a graph based geometry repair algorithm is used to repair the geometry by adding minimum possible segments to the Delaunay triangulation mesh to form a volume connection set. The details on the related graph based repair can be found in [56] on water distribution networks.

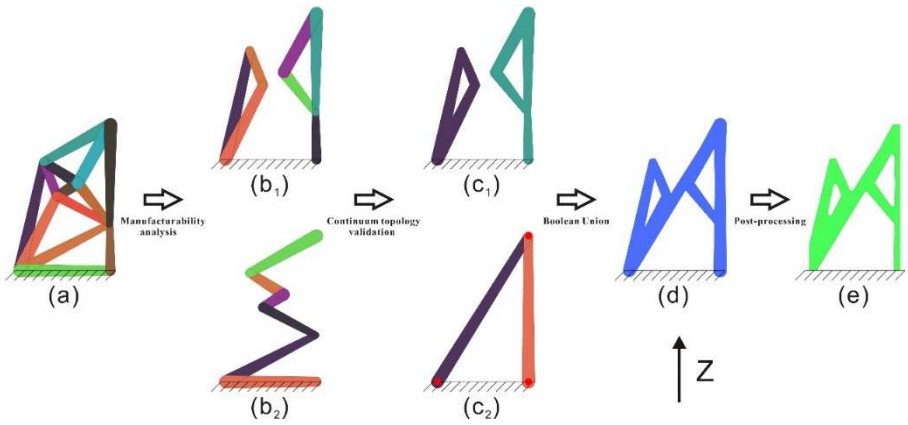

Fig. 17. Continuum topology validation: (a) original primitive units obtained by Delaunay triangulation skeletons; (b_1) manufacturable primitive units; (b_2) unmanufacturable primitive units; (c_1) manufacturable primitive units after Boolean union; (c_2) pre-defined manufacturable & repaired geometry; (d) geometry of c_1 and c_2 after Boolean union; (e) final qualified geometry after post-processing.

An example of continuum topology validation is exhibited in Fig. 17. Fig. 17(a) represents the original primitive units via the Delaunay triangulation algorithm. The topology structures in Fig. 17(b_1) and (b_2) are

manufacturable and unmanufacturable primitive units after manufacturability analysis, respectively. The topology structure shown in Fig. 17(c_1) is checked as an invalid continuum structure. Hence, a continuum geometry repair operator is required to repair the invalid structure by adding some primitive units to connect all printable units. Initially, it is mandatory to find a connection strategy to connect all the fixed nodes and ensure the manufacturability of these primitives. Such a connection strategy among fixed nodes should guarantee that repair segments obtain all fixed nodes. The inconsistent geometries (Fig. 17(c_1)) are connected to repaired segments (Fig. 17(c_2)). The repaired geometries via the Boolean union and post-processing are shown in Fig. 17(d) and (e), respectively. After the continuum geometry repair operation, a final qualified AM-oriented continuum topology is formed.

3.2 Alternative design solution generation and optimization

As introduced above, a generative design in structural design mainly uses evolutionary algorithms to populate numerous alternative solutions to respond to predefined objectives and constraints. In this paper, in order to conduct multi-objective optimization and generate a large number of alternative topology structures, a multi-objective evolutionary algorithm, NSGA-II [57], is adopted to obtain a set of Pareto-optimal solutions. NSGA-II is a very popular algorithm and it has been demonstrated as one of the most efficient algorithm for the most efficient algorithms for multi-objective optimization on many benchmark problems. The algorithm flowchart is presented in Fig. 18.

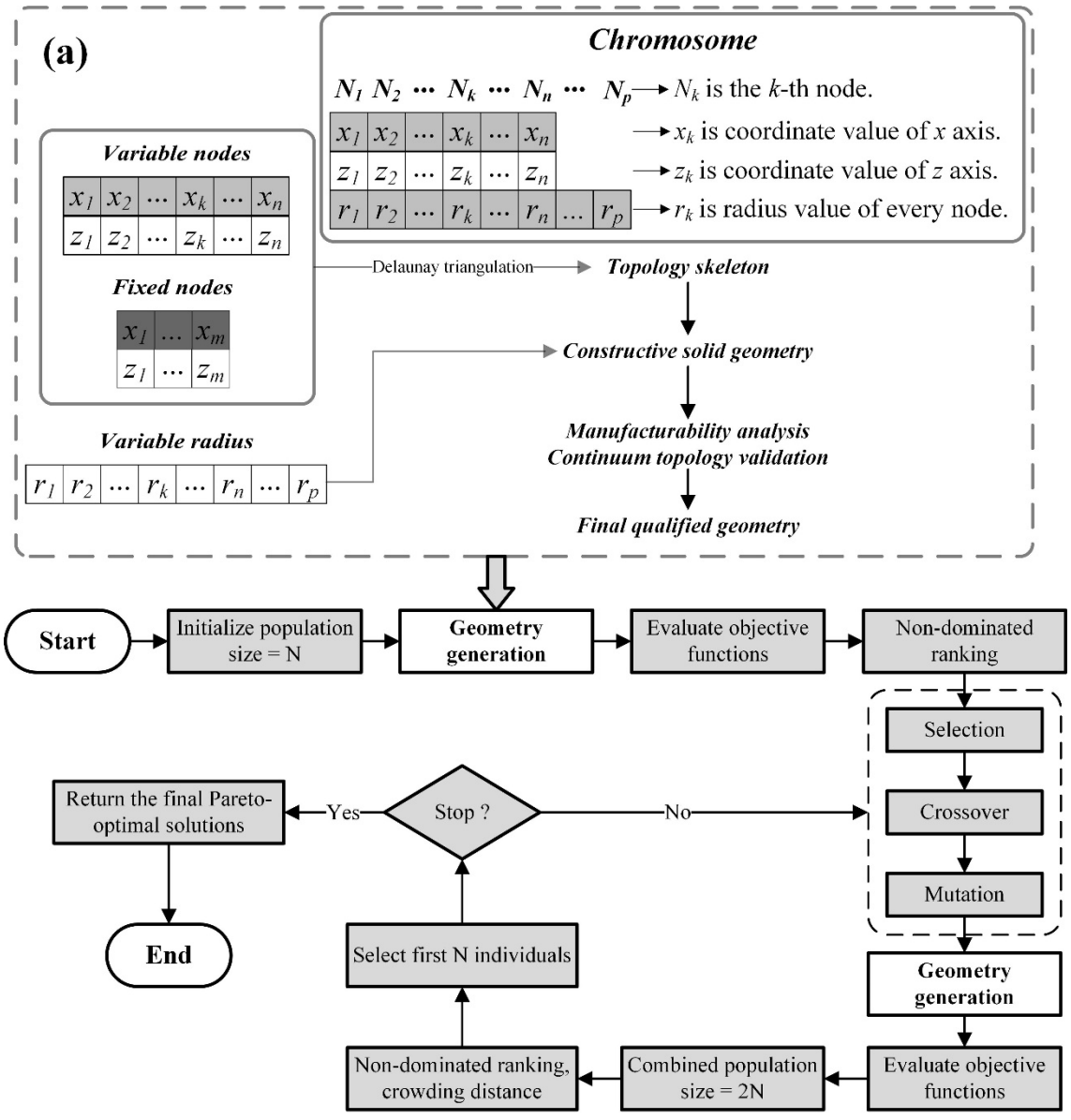

Fig. 18. Flowchart of a Pareto-optimal solutions search

In Fig. 18(a), the relationship between chromosome and topology geometry is set out to explain the geometry generation. The topology skeleton is defined by the position of variable and fixed nodes on the XOZ plane using the Delaunay triangulation algorithm. Three types of variables are set for constructing topology geometry. Manufacturability analysis and continuum topology validation can enable the final geometry to be qualified. Two objective functions are defined to minimize the volume and compliance. 2D triangular mesh is used to complete the finite element analysis. The GA parameters and its coding are also shown in Fig. 18(a).

4. Case study

In this section, bi-objective optimization for compliance minimization problems is selected to demonstrate the performance of the proposed method. Parameters in the standard NSGA-II algorithm are defined in Tab. 2. For all cases, the values of the crossover probability of 0.9 and the crossover distribution index are set as 0.9 and 20 respectively, and a mutation probability of 0.3 and a mutation distribution index of 20 are adopted. In order to solve the compliance minimization problem volume V and compliance C are minimized simultaneously. The optimization problem is formulated as:

$$Min: \begin{cases} f_1 = V/V_{\max} \\ f_2 = u^T K u \end{cases} \tag{10}$$

Where V is the volume of the final geometry, $V_{\max}$ is the volume of the design domain, u is the displacement vector, K is the global stiffness matrix. 2D triangular meshing technique is applied to mesh the geometry and calculate the compliance.

Tab. 2. Parameters definition of NSGA-II algorithm

Option	Description
Crossover probability	0.9
Crossover distribution index	20
Mutation probability	0.3
Mutation distribution index	20

4.1 Asymmetric design domain case

The design domain and boundaries for the cantilever beam problem is defined by using a previous build orientation method in Fig. 19. The design domain is $3L \times L$ and a point force F is applied to the boundary. Tab. 3 lists a series of parameters used in the problem.

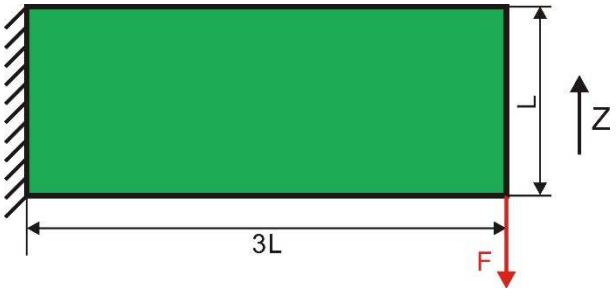

Fig. 19. Design domain for case 1

Tab. 3 Parameters used in the cantilever beam problem

Option	**Description**
The number of fixed nodes (m)	3
The number of variable nodes (p)	15
Population size	100
Generations	500
Force (F)	100 N
Radius range (r)	0.4-3 mm

Maximum overhang distance (O_M)	2 mm
Maximum overhang angle (θ)	45°

According to the proposed geometry representation method, three fixed nodes are defined on the load and support boundary, and seven variable nodes are applied in the design domain. Subsequently, a pre-optimal build orientation is determined in order to obtain more Delaunay triangulation skeletons that meet the manufacturing constraints (as shown in Fig. 20(a)) The number of adaptive variable nodes are n $(1 \le n \le p)$. Hence, the number of variable is $6 \le 2n+(m+n) \le 48$. The range of x and z position variable varies from 0 to 20 and 0 to 60, respectively. Fixed nodes are defined at (0, 0), (0, 60) and (20, 60). The sorting of nodes is shown in Fig. 20(b). A commonly accepted value of the maximum overhang angle is 40°-50°. In this case, the maximum overhang angle and distance are defined as 45° and 2mm respectively.

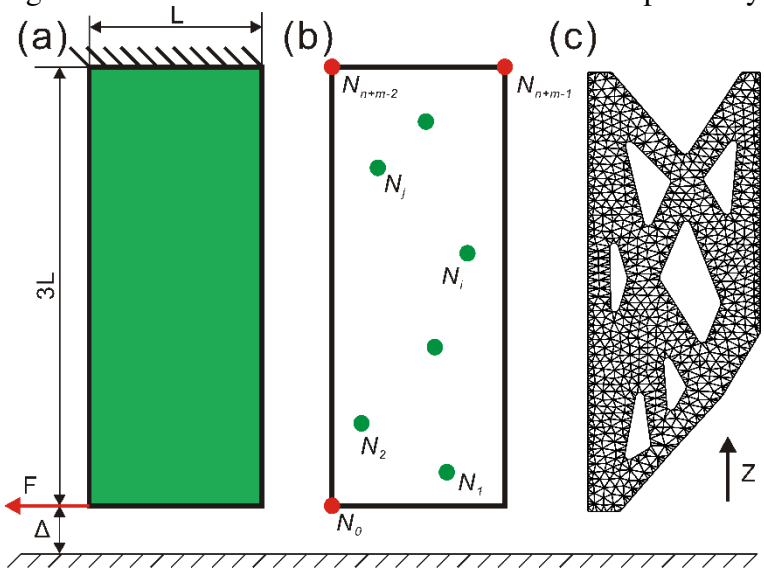

Fig. 20. (a). the optimized build orientation; (b). adaptive node definition; (c). 2D triangular meshing.

The initial parameter of the proposed GD method is set as: population size, 100; stop criterion of the optimization, 500 generations. The Pareto-optimal solutions obtained for the optimization problem are indicated in Fig. 21. Each point on the Pareto front represents a design structure for the corresponding volume ratio.

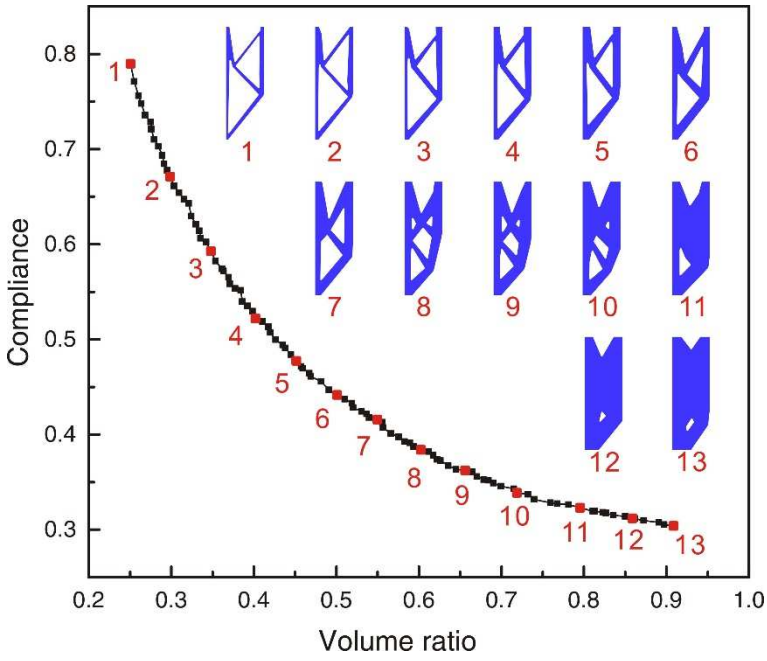

Fig. 21. Pareto-optimal solutions for the CSG-based generative design method

It is assumed that solutions with a volume ratio less than 0.25 are infeasible. In Fig. 21, thirteen sample optimal solutions for different volume ratios on the Pareto front are selected and corresponding structures are indicated. Sample 1 to 7 have a similar shape, but variations in the radius provide differences in the objective values. The evolution of the structure is illustrated in Fig. 22. Six different generations are marked and the corresponding volume ratios are also shown.

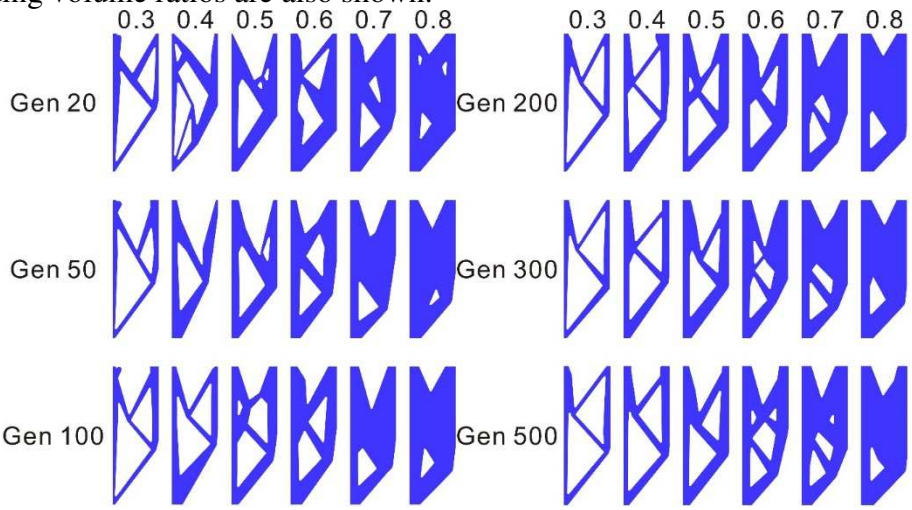

Fig. 22. Evolutionary trend of Pareto-optimal solutions

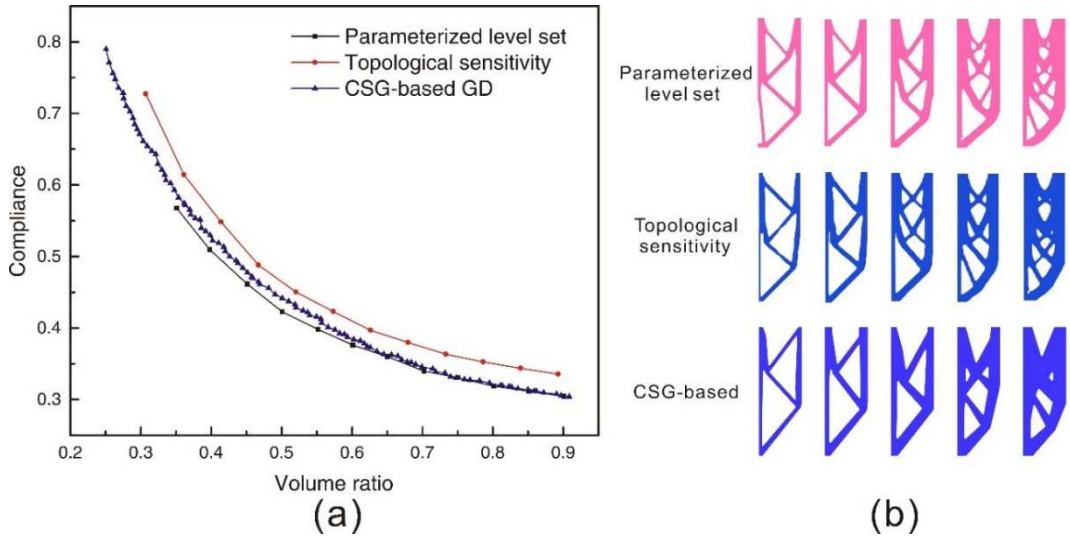

Fig. 23. The Pareto-optimal curves and corresponding sample solutions for three methods

Fig. 23 compares the results of the proposed method with that of two other methods in literature. In [58], the topological sensitivity method was used to generate Pareto-optimal topologies. However, the author focuses on the material distribution and ignores the manufacturability. Nevertheless, the proposed method in this paper still shows a good performance. In [59], a parameterized level set method is applied to minimize the compliance of a single-objective two-dimensional (2D) structure problem. The level set method can maintain a smooth level set function and does not need to implement any filter during the optimization process. Though level set method provides a slightly better trade-off front than that of the proposed CGS-based GD method, it needs to make multiple runs with different volume constraints each time and does not consider manufacturing constraints a problem. The results of the level set are not qualified AM design solutions. Compared to these gradient-based topology optimization methods, the proposed method utilizes a small number of design variables and populates a set of qualified and relatively optimal candidate solutions on the Pareto front. More importantly, all the generated alternative solutions are valid solutions for the AM process, which is critical for industrial design practice in AM.

Most research in literature has suggested that the maximum overhang angle for L-PBF was 45°. However, this angle depends on the parameter setting of specific AM machines. Hence, the design optimization method should have the capability to include this flexibility. Due to the parametric control for all variables,

the proposed method is convenient in that it adjusts all the parameters according to the needs of specific AM processes. In order to further verify the effectiveness of the proposed CSG-based method, different maximum manufacturing overhang angle constraints are investigated. Fig. 24 gives a part of the Pareto-optimal solutions for two maximum overhang angles, 60° and 75°, respectively.

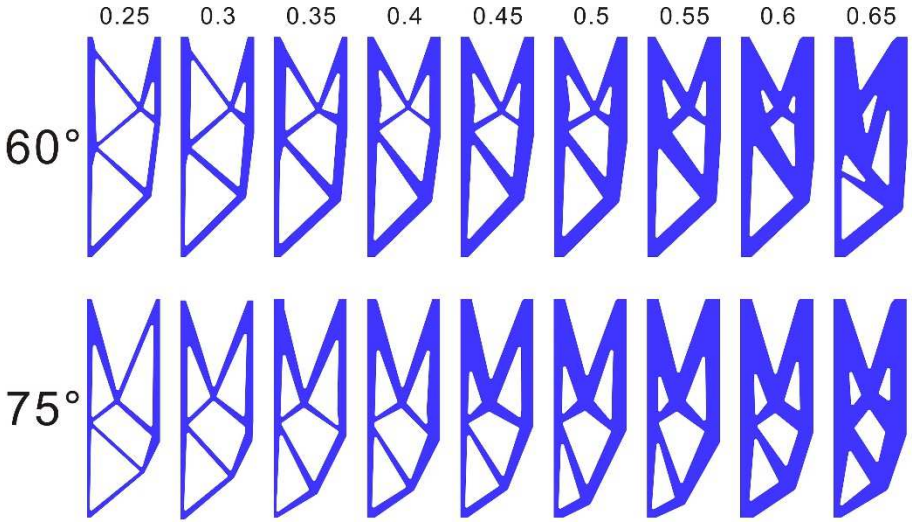

Fig. 24. Pareto-optimal solutions for different overhang angle constraints

4.2 Symmetric design domain case

In topology optimization problem, design domain with symmetric boundary conditions is often encountered. To show the effectiveness of the proposed method, a symmetry beam problem is tested. To solve this problem, a simple skeleton mirroring method is designed to obtain symmetry skeletons as an adaption of the Delaunay triangulation algorithm. According to the proposed method framework above, the pre-optimal build orientation definition and the fixed and variable nodes determination results are presented in Fig. 25.

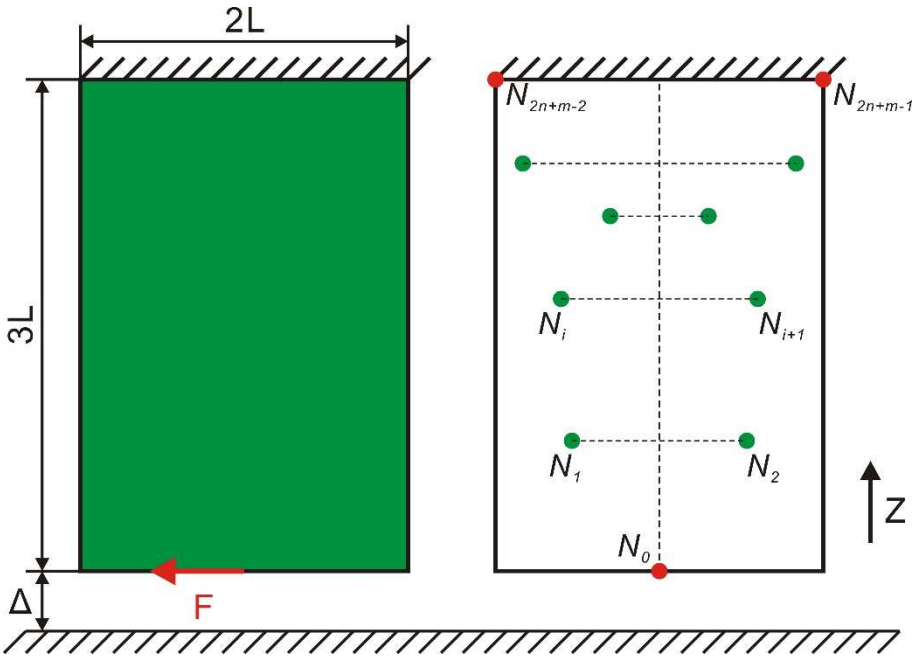

Fig. 25. Design domain and adaptive node definition for case 2

In this case, three fixed nodes and fifteen variable nodes are defined and the corresponding mirror nodes are generated as shown in Fig. 26(a). A Delaunay triangulation skeleton is represented by a set of connected nodes. In Fig. 26(b), the skeletons that do not meet the symmetry condition are colored in red. The symmetry problem can be solved by mirroring the skeleton on the other side. The mirror skeletons are

shown in blue in Fig. 26(c). The final skeleton is composed of the original skeleton and mirror lines. Once the symmetry skeleton is obtained, the subsequent operations are the same, as shown in Fig. 8.

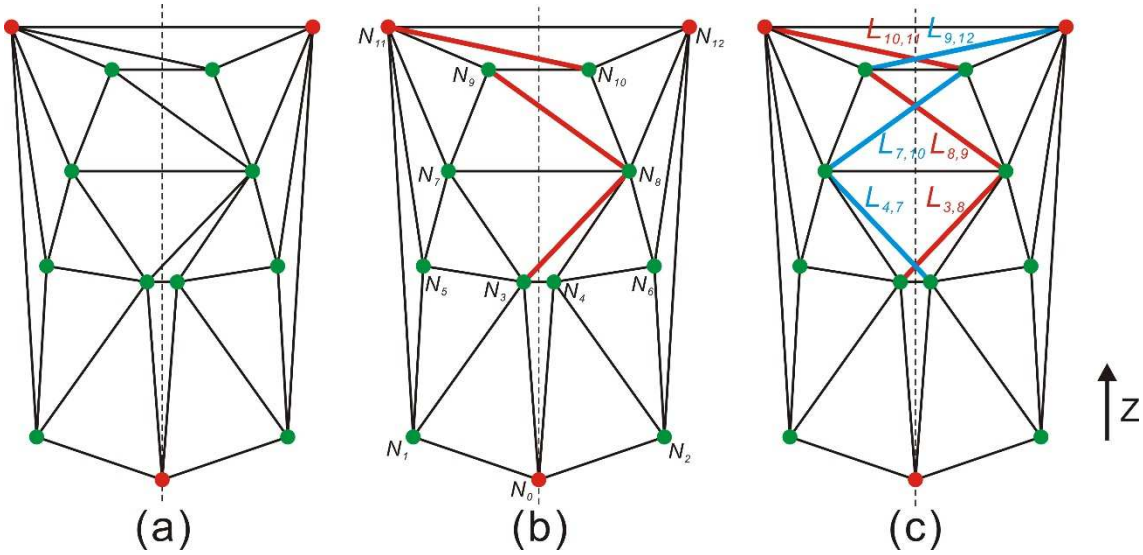

Fig. 26. Symmetry skeleton for the proposed CSG-based generative design method

Regarding the symmetry problem, fixed nodes are defined at the positions of (20, 0), (0, 60) and (40, 60). The number of adaptive variable nodes is n $(1 \le n \le p)$. Hence, the number of all variables is $6 \le 2n + (m-1+n) \le 47$. The range of x and z position variable varies from 0 to 20 and 0 to 60, respectively. The maximum overhang angle and distance are also defined as 45° and 2mm. Fig. 27 captures the Pareto-optimal solutions obtained by the proposed CSG-based generative design method. Solution 2 to 9 have a similar shape with different widths. With the increase in the width of primitives, the internal gaps gradually decrease. In solution 11, the internal holes/cavities disappear.

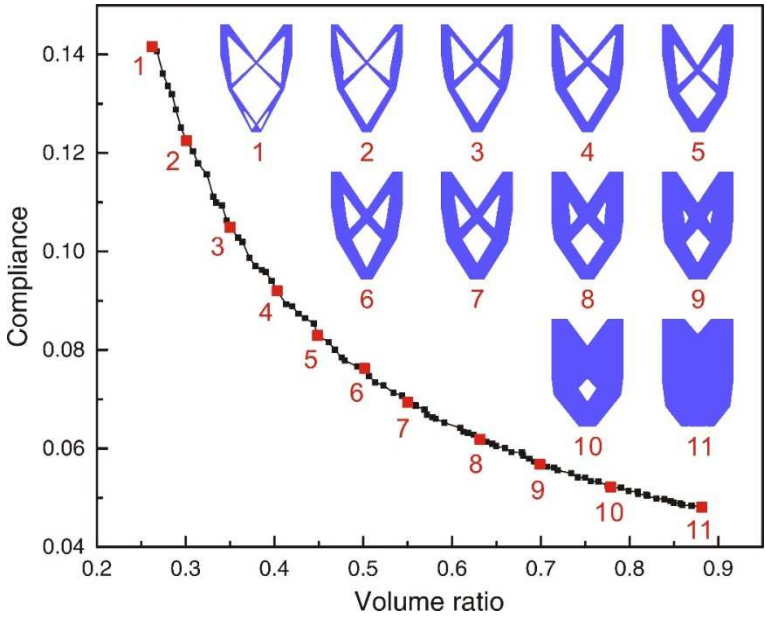

Fig. 27. Pareto-optimal solutions for case 2

To further demonstrate the proposed method, the results obtained are compared with that of two other existing methods. The Pareto-optimal curves and the corresponding structure of three methods are shown below in Fig. 28. As shown in Fig. 28(a), three Pareto-optimal curves have the same trend. The CSG-GD method and topological sensitivity perform similarly when the volume ratio is less than 0.3 or more than 0.45. However, the parameterized level set method has a better Pareto front on average. When the volume ratio is higher than 0.65, three methods exhibit similar Pareto-optimal values.

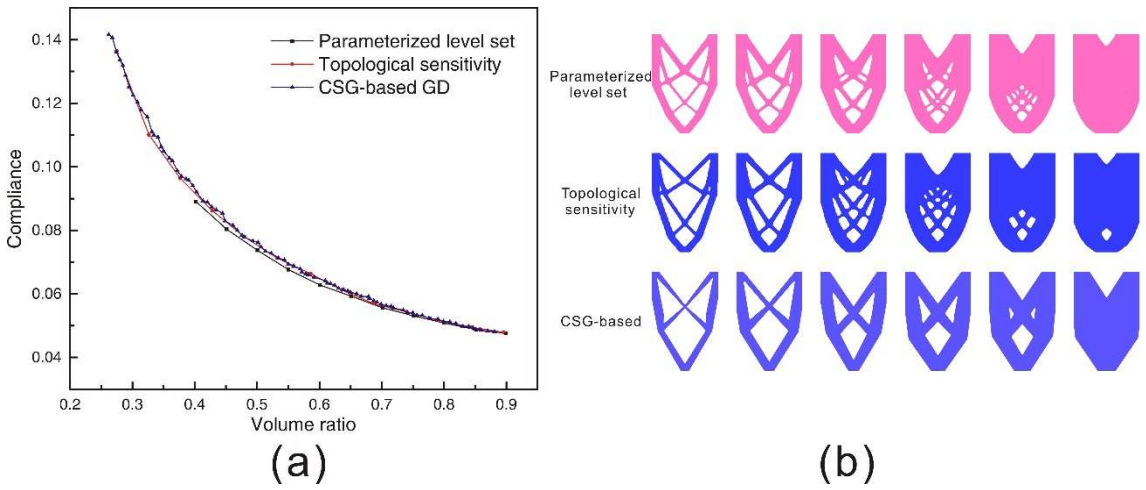

Fig. 28. The Pareto-optimal curves for three methods in symmetry beam problem

As discussed above, though the proposed CSG-based GD method does not exhibit a better performance than that of the level set method, it better integrates AM manufacturing constraints into generative design algorithm. In addition, the proposed method has the potential to achieve a good compromise for multi-objective optimization problems via the providing of a set of qualified alternative solutions to facilitate decision-making for the designers. Generally, compared to the sensitivity-based TO method, the proposed approach has a better trade-off in Pareto-optimal tracing and has a similar performance to that of the level set method. Due to the consideration of many manufacturing constraints in AM, the proposed method can better exert the potential of AM and generate qualified design solutions.

To validate the manufacturability of the obtained Pareto optimal solutions, several Pareto solutions of the two cases were selected and printed by an SLA (Stereolithography) machine. The printing sizes were set as $20\times60\times5$mm and $40\times60\times5$mm respectively for the asymmetric design domain case and the symmetric design domain case respectively. Figure 29 presents the printing results, which shows the structures are self-supported and there is no failure in the printing. Similarly, other AM process, e.g. SLM, can also be used for evaluation, but we only need to reset some of the manufacturing constraints' values, such as the maximum bridge length of the AM process, in the TO procedure.

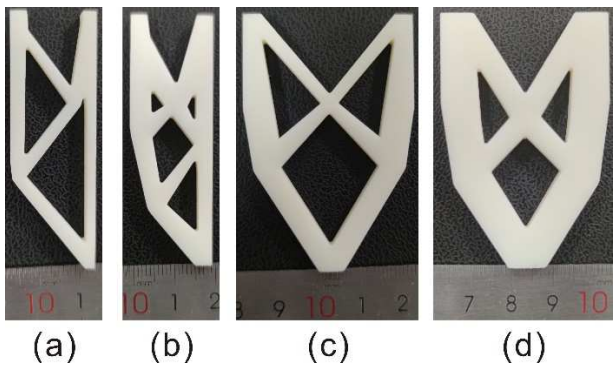

Fig. 29. Asymmetric design domain case: (a). volume ratio = 0.4; (b). volume ratio = 0.6; symmetric design domain case: (c). volume ratio = 0.4; (d). volume ratio = 0.6.

5. Conclusions and perspectives

In this paper, a new CSG-based generative design method is proposed to generate and search for optimal qualified AM design solutions. General AM manufacturing constraints are analyzed and modelled to support practical DFAM needs. It differs from the traditional TO method based on gradient information, as it has the potential to deal with manufacturing constraints through an explicit geometrical representation. The main contribution of this work is the introduction of a CSG geometry representation for topology optimization for AM and the realization of parametric control of explicit geometries with smooth boundaries. The application

of geometric shape control points in the TO operation can greatly reduce the number of design variables and release the potential of evolutionary algorithm-based TO methods. Furthermore, a major advantage of the proposed method is to obtain strong convex Pareto sets, which are qualified design solutions for conflicting objective functions. Hence, a Pareto-optimal set can represent the trade-off for further decision making when compromise should be made with diverse preferences in specific applications.

Currently, the proposed method only adopts the Delaunay triangulation mesh to generate topology skeleton and defines quite simple primitive shapes. Therefore, to further improve this method, more skeleton generation methods should be investigated and the NURBS-based unit shape definition method could be explored, which may be helpful in embedding more complex AM manufacturing constraints. For some non-convex design domains with complex boundaries, the proposed method would possibly encounter some difficulty. To reduce the complexity, a set of geometric operations could be used to decompose the design domain into multiple simpler convex geometries. In the authors' future work, complex design domains will be explored to extend the proposed method and isogeometric analysis (IGA) will be applied to the framework. Then, a three-dimensional generative design method will be extended. To avoid the emergence of closed internal holes, open lattice unit cells will be applied to fill into the 3D structure. In addition, more manufacturing constraints of hybrid AM process will be considered to support the design for hybrid AM process.

References

[1] A. E2987/E2987M, Standard Terminology for Additive Manufacturing, (2016).
[2] D.W. Rosen, Research supporting principles for design for additive manufacturing, Virtual and Physical Prototyping 9(4) (2014) 225-232.
[3] N. Lebaal, Y. Zhang, F. Demoly, S. Roth, S. Gomes, A. Bernard, Optimised lattice structure configuration for additive manufacturing, CIRP Annals 69(1) (2019) 117-120.
[4] M.K. Thompson, G. Moroni, T. Vaneker, G. Fadel, R.I. Campbell, I. Gibson, A. Bernard, J. Schulz, P. Graf, B. Ahuja, F. Martina, Design for Additive Manufacturing: Trends, opportunities, considerations, and constraints, CIRP Annals 65(2) (2016) 737-760.
[5] Y. Xiong, P.L.T. Duong, D. Wang, S.-I. Park, Q. Ge, N. Raghavan, D.W. Rosen, Data-Driven Design Space Exploration and Exploitation for Design for Additive Manufacturing, Journal of Mechanical Design 141(10) (2019).
[6] D.W. Rosen, A review of synthesis methods for additive manufacturing, Virtual and Physical Prototyping 11(4) (2016) 305-317.
[7] T. Vaneker, A. Bernard, G. Moroni, I. Gibson, Y. Zhang, Design for additive manufacturing: Framework and methodology, CIRP Annals (2020).
[8] O. Sigmund, On the usefulness of non-gradient approaches in topology optimization, Structural and Multidisciplinary Optimization 43(5) (2011) 589-596.
[9] Y. Tang, Y.F. Zhao, A survey of the design methods for additive manufacturing to improve functional performance, Rapid Prototyping Journal 22(3) (2016) 569-590.
[10] P.W. Mani Mahesh, and Haeseong Jee, Design rules for additive manufacturing: a catrgorization, ASME 2017 International Design Engineering Technical Conference and Computers and Information in Engineering Conference (2017).
[11] Y. Zhang, A. Bernard, R.K. Gupta, R. Harik, Evaluating the Design for Additive Manufacturing: A Process Planning Perspective, Procedia CIRP 21 (2014) 144-150.
[12] M. Leary, L. Merli, F. Torti, M. Mazur, M. Brandt, Optimal topology for additive manufacture: A method for enabling additive manufacture of support-free optimal structures, Materials & Design 63 (2014) 678-690.
[13] A.T. Gaynor, N.A. Meisel, C.B. Williams, J.K. Guest, Topology Optimization for Additive Manufacturing: Considering Maximum Overhang Constraint, 15th AIAA/ISSMO Multidisciplinary Analysis and Optimization Conference, 2014.
[14] A.T. Gaynor, J.K. Guest, Topology optimization considering overhang constraints: Eliminating sacrificial support material in additive manufacturing through design, Structural and Multidisciplinary Optimization 54(5) (2016) 1157-1172.
[15] M. Langelaar, An additive manufacturing filter for topology optimization of print-ready designs, Structural and Multidisciplinary Optimization 55(3) (2016) 871-883.
[16] M. Langelaar, Topology optimization of 3D self-supporting structures for additive manufacturing, Additive Manufacturing 12 (2016) 60-70.
[17] M. Langelaar, Combined optimization of part topology, support structure layout and build orientation for additive manufacturing, Structural and Multidisciplinary Optimization 57(5) (2018) 1985-2004.
[18] B. Barroqueiro, A. Andrade-Campos, R.A.F. Valente, Designing Self Supported SLM Structures via Topology Optimization, Journal of Manufacturing and Materials Processing 3(3) (2019).

[19] Y.-F. Fu, B. Rolfe, L.N.S. Chiu, Y. Wang, X. Huang, K. Ghabraie, Design and experimental validation of self-supporting topologies for additive manufacturing, Virtual and Physical Prototyping 14(4) (2019) 382-394.
[20] Y.-F. Fu, B. Rolfe, L.N.S. Chiu, Y. Wang, X. Huang, K. Ghabraie, Parametric studies and manufacturability experiments on smooth self-supporting topologies, Virtual and Physical Prototyping 15(1) (2019) 22-34.
[21] C.J. Thore, H.A. Grundström, B. Torstenfelt, A. Klarbring, Penalty regulation of overhang in topology optimization for additive manufacturing, Structural and Multidisciplinary Optimization (2019).
[22] M.L. Zhao Dengyang, and Yusheng Liu, Self-supporting topology optimization for additive manufacturing, arXiv 1708.07364 (2017).
[23] X. Guo, W. Zhang, W. Zhong, Doing Topology Optimization Explicitly and Geometrically—A New Moving Morphable Components Based Framework, Journal of Applied Mechanics 81(8) (2014).
[24] W. Zhang, J. Yuan, J. Zhang, X. Guo, A new topology optimization approach based on Moving Morphable Components (MMC) and the ersatz material model, Structural and Multidisciplinary Optimization 53(6) (2015) 1243-1260.
[25] W. Zhang, J. Chen, X. Zhu, J. Zhou, D. Xue, X. Lei, X. Guo, Explicit three dimensional topology optimization via Moving Morphable Void (MMV) approach, Computer Methods in Applied Mechanics and Engineering 322 (2017) 590-614.
[26] G. Allaire, C. Dapogny, R. Estevez, A. Faure, G. Michailidis, Structural optimization under overhang constraints imposed by additive manufacturing technologies, Journal of Computational Physics 351 (2017) 295-328.
[27] Y. Wang, J. Gao, Z. Kang, Level set-based topology optimization with overhang constraint: Towards support-free additive manufacturing, Computer Methods in Applied Mechanics and Engineering 339 (2018) 591-614.
[28] X. Guo, J. Zhou, W. Zhang, Z. Du, C. Liu, Y. Liu, Self-supporting structure design in additive manufacturing through explicit topology optimization, Computer Methods in Applied Mechanics and Engineering 323 (2017) 27-63.
[29] G.R. Zavala, A.J. Nebro, F. Luna, C.A. Coello Coello, A survey of multi-objective metaheuristics applied to structural optimization, Structural and Multidisciplinary Optimization 49(4) (2013) 537-558.
[30] J.E.S. A.E. Eiben, Introduction to Evolutionary Computing Second Edition, Springer-Verlag Berlin Heidelberg2007.
[31] M.O. Nikola Aulig, Evolutionary computation for topology optimization of mechanical structures An overview of representations, in: IEEE (Ed.) 2016 IEEE Congress on Evolutionary Computation, 2016.
[32] D. Guirguis, C.A.C. Coello, K. Saitou, N. Aulig, R. Picelli, B. Zhu, Y. Zhou, W. Vicente, F. Iorio, M. Olhofer, W. Matusik, Evolutionary Black-box Topology Optimization: Challenges and Promises, IEEE Transactions on Evolutionary Computation (2019) 1-1.
[33] B.R. Bielefeldt, E. Akleman, G.W. Reich, P.S. Beran, D.J. Hartl, L-System-Generated Mechanism Topology Optimization Using Graph-Based Interpretation, Journal of Mechanisms and Robotics 11(2) (2019).
[34] B.R. Bielefeldt, G.W. Reich, P.S. Beran, D.J. Hartl, Development and validation of a genetic L-System programming framework for topology optimization of multifunctional structures, Computers & Structures 218 (2019) 152-169.
[35] N. Aulig, M. Olhofer, Neuro-evolutionary topology optimization of structures by utilizing local state features, Proceedings of the 2014 conference on Genetic and evolutionary computation - GECCO '14, 2014, pp. 967-974.
[36] K.O. Stanley, Compositional pattern producing networks: A novel abstraction of development, Genetic Programming and Evolvable Machines 8(2) (2007) 131-162.
[37] H.H.a.M. Schoenauer, Topological optimum design with Evolutionary Algorithms, Journal of Convex Analysis 9 (2002) 503-518.
[38] F. Ahmed, K. Deb, B. Bhattacharya, Structural topology optimization using multi-objective genetic algorithm with constructive solid geometry representation, Applied Soft Computing 39 (2016) 240-250.
[39] A. Pandey, R. Datta, B. Bhattacharya, Topology optimization of compliant structures and mechanisms using constructive solid geometry for 2-d and 3-d applications, Soft Computing 21(5) (2015) 1157-1179.
[40] J.A. Madeira, H.C. Rodrigues, H. Pina, Multiobjective topology optimization of structures using genetic algorithms with chromosome repairing, Structural and Multidisciplinary Optimization 32(1) (2006) 31-39.
[41] Y. Sato, K. Izui, T. Yamada, S. Nishiwaki, Pareto frontier exploration in multiobjective topology optimization using adaptive weighting and point selection schemes, Structural and Multidisciplinary Optimization 55(2) (2016) 409-422.
[42] A. Cardillo, G. Cascini, F.S. Frillici, F. Rotini, Multi-objective topology optimization through GA-based hybridization of partial solutions, Engineering with Computers 29(3) (2012) 287-306.
[43] V. Singh, N. Gu, Towards an integrated generative design framework, Design Studies 33(2) (2012) 185-207.
[44] I. Jowers, C. Earl, G. Stiny, Shapes, structures and shape grammar implementation, Computer-Aided Design 111 (2019) 80-92.
[45] B. Bochenek, K. Tajs-Zielińska, Novel local rules of cellular automata applied to topology and size optimization, Engineering Optimization 44(1) (2012) 23-35.
[46] V. Dhokia, W.P. Essink, J.M. Flynn, A generative multi-agent design methodology for additively manufactured parts inspired by termite nest building, CIRP Annals 66(1) (2017) 153-156.
[47] W.P. Essink, J.M. Flynn, S. Goguelin, V. Dhokia, Hybrid Ants: A New Approach for Geometry Creation for Additive and Hybrid Manufacturing, Procedia CIRP 60 (2017) 199-204.
[48] S. Oh, Y. Jung, S. Kim, I. Lee, N. Kang, Deep Generative Design: Integration of Topology Optimization and Generative Models, Journal of Mechanical Design 141(11) (2019).

[49] Y. Zhang, A. Bernard, R. Harik, K.P. Karunakaran, Build orientation optimization for multi-part production in additive manufacturing, Journal of Intelligent Manufacturing 28(6) (2015) 1393-1407.
[50] Y. Zhang, R. Harik, G. Fadel, A. Bernard, A statistical method for build orientation determination in additive manufacturing, Rapid Prototyping Journal (2018).
[51] Y. Zhang, W. De Backer, R. Harik, A. Bernard, Build Orientation Determination for Multi-material Deposition Additive Manufacturing with Continuous Fibers, Procedia CIRP 50 (2016) 414-419.
[52] J. Olsen, I.Y. Kim, Design for additive manufacturing: 3D simultaneous topology and build orientation optimization, Structural and Multidisciplinary Optimization (2020).
[53] Y. Zhang, Z. Wang, Y. Zhang, S. Gomes, A. Bernard, Bio-inspired generative design for support structure generation and optimization in Additive Manufacturing (AM), CIRP Annals (2020).
[54] D. Thomas, A deep dive into metal 3D printing, Laser 3D Manufacturing VI, International Society for Optics and Photonics, 2019.
[55] H. Yu, J. Liu, Self-Support Topology Optimization With Horizontal Overhangs for Additive Manufacturing, Journal of Manufacturing Science and Engineering 142(9) (2020).
[56] S. Bureerat, K. Sriworamas, Simultaneous topology and sizing optimization of a water distribution network using a hybrid multiobjective evolutionary algorithm, Applied Soft Computing 13(8) (2013) 3693-3702.
[57] A.P. Kalyanmoy Deb, Sameer Agarwal, and T. Meyarivan, A fast and elitist multiobjective genetic algorithm: NSGA-II, IEEE Transactions on Evolutionary Computation Vol. 6, No. 2 (2002).
[58] K. Suresh, A 199-line Matlab code for Pareto-optimal tracing in topology optimization, Structural and Multidisciplinary Optimization 42(5) (2010) 665-679.
[59] P. Wei, Z. Li, X. Li, M.Y. Wang, An 88-line MATLAB code for the parameterized level set method based topology optimization using radial basis functions, Structural and Multidisciplinary Optimization 58(2) (2018) 831-849.